Molecular Therapy
Methods & Clinical Development
Original Article

Comparative dose effectiveness of intravenous and intrathecal AAV9.CB7.hIDS, RGX-121, in mucopolysaccharidosis type II mice

Miles C. Smith,[1] Lalitha R. Belur,[1] Andrea D. Karlen,[1] Olivia Erlanson,[1] Justin Furcich,[2] Troy C. Lund,[2] Davis Seelig,[3] Kelley F. Kitto,[4] Carolyn A. Fairbanks,[4] Kwi Hye Kim,[5] Nick Buss,[5] and R. Scott McIvor[1]

[1]Center for Genome Engineering, Department of Genetics, Cell Biology and Development, University of Minnesota, Minneapolis, MN 55455, USA; [2]Department of Pediatrics, University of Minnesota, Minneapolis, MN 55455, USA; [3]Comparative Pathology Shared Resource, University of Minnesota, St. Paul, MN 55455, USA; [4]Department of Pharmaceutics, University of Minnesota, Minneapolis, MN 55455, USA; [5]REGENXBIO Inc., Rockville, MD 20850, USA

Mucopolysaccharidosis type II (MPS II) is an X-linked recessive lysosomal disease caused by iduronate-2-sulfatase (IDS) deficiency, leading to accumulation of glycosaminoglycans (GAGs) and the emergence of progressive disease. Enzyme replacement therapy is the only currently approved treatment, but it leaves neurological disease unaddressed. Cerebrospinal fluid (CSF)-directed administration of AAV9.CB7.hIDS (RGX-121) is an alternative treatment strategy, but it is unknown if this approach will affect both neurologic and systemic manifestations. We compared the effectiveness of intrathecal (i.t.) and intravenous (i.v.) routes of administration (ROAs) at a range of vector doses in a mouse model of MPS II. While lower doses were completely ineffective, a total dose of 1×10^9 gc resulted in appreciable IDS activity levels in plasma but not tissues. Total doses of 1×10^{10} and 1×10^{11} gc by either ROA resulted in supraphysiological plasma IDS activity, substantial IDS activity levels and GAG reduction in nearly all tissues, and normalized zygomatic arch diameter. In the brain, a dose of 1×10^{11} gc i.t. achieved the highest IDS activity levels and the greatest reduction in GAG content, and it prevented neurocognitive deficiency. We conclude that a dose of 1×10^{10} gc normalized metabolic and skeletal outcomes, while neurologic improvement required a dose of 1×10^{11} gc, thereby suggesting the prospect of a similar direct benefit in humans.

INTRODUCTION

Mucopolysaccharidosis type II (MPS II or Hunter syndrome) is an X-linked recessive lysosomal disease that affects approximately 1:160,000 male births.[1] The disease is caused by mutation in the *IDS* gene, which leads to deficiency of iduronate-2-sulfatase (IDS). IDS is required for the stepwise degradation of glycosaminoglycans (GAGs) heparan sulfate and dermatan sulfate.[2] Insufficient IDS thus leads to lysosomal accumulation of fully or partially undegraded GAGs in most tissues, including cardiac, skeletal, and nervous tissue. Patients with MPS II manifest organomegaly, joint stiffness, arthropathy, hearing loss, cardiopulmonary dysfunction, and skeletal dysplasias.[3] In addition to peripheral disease symptoms, two-thirds of patients exhibit central nervous system (CNS) manifestations that begin around the age of 2 years. This neuronopathic form of MPS II includes aggressive behavioral problems, seizures, developmental delay, neurocognitive decline, and death by adolescence.[2–5]

Enzyme replacement therapy (ERT), intravenously (i.v.) administered recombinant idursulfase (IDS), is the current standard of care for MPS II.[6–8] Both non-neuronopathic and neuronopathic forms of MPS show benefit from ERT in the periphery, such as reduced urine GAG excretion, reduced organomegaly, and improved walking performance.[9,10] ERT can thus manage some aspects of the disease with weekly infusions, but some peripheral and all neurological disease manifestations are left unaddressed. Patients followed for 9 years on ERT did not improve in respiratory, skeletal, or CNS outcomes.[11] It is widely held that ERT provides no CNS benefit for neuronopathic MPS II because the administered enzyme does not cross the blood-brain barrier (BBB).[12] A recent clinical evaluation of intrathecally (i.t.) administered ERT failed to stabilize neurocognitive function in patients.[13] ERT is also problematic with regard to high cost and time-consuming weekly infusions. Due to its effectiveness in other lysosomal diseases such as MPS I, allogeneic hematopoietic stem cell transplantation (HSCT) has also been considered as a treatment for MPS II. However, due to early reports of uncertain CNS benefit and transplant complications, HSCT is not currently recommended for MPS II.[14] Although more recent reports on HSCT for MPS II have shown some neurologic benefit, so far there is insufficient and variable clinical outcome.[15–17] There is thus an unmet need for treatment that can overcome the limitations of those currently available for MPS II, particularly the neuronopathic form of the disease.

Received 27 June 2023; accepted 24 January 2024;
https://doi.org/10.1016/j.omtm.2024.101201.

Correspondence: R. Scott McIvor, Center for Genome Engineering, Department of Genetics, Cell Biology and Development, University of Minnesota, Minneapolis, MN 55455, USA.
E-mail: mcivo001@umn.edu

The monogenic nature of MPS II supports anticipation that metabolic correction will be achievable by supplying a functional copy of the *IDS* sequence via gene transfer. In addition, cells supplied with a functional gene copy can secrete enzyme via the mannose-6-phosphate pathway to metabolically cross-correct other defective cells.[18] For *in vivo* gene transfer, adeno-associated virus (AAV) vectors have several advantageous properties for treating lysosomal diseases in general, such as a variety of tropisms, the potential for strong and lasting expression, and lack of natural pathogenicity.[19–22] AAV serotype 9 (AAV9) has been of particular interest for MPS II gene therapy owing to its neurotropic properties and potential for systemic transduction.[23,24] Delivery of AAV for MPS II has been accomplished through both systemic and CNS-directed routes of administration (ROAs) in MPS II mice. The earliest reports consisted of systemically administered AAV2 vector, showing correction of skeletal and locomotor abnormalities.[25,26] More recently, self-complementary (sc) AAV9 was introduced i.v. showing brain IDS activity, brain GAG reduction, and improved neurobehavior using vector doses between 2.5×10^{12} genome copies (gc) and 2×10^{13} gc.[27] Several preclinical studies have explored CSF-directed AAV9 administration via either intracisternal or intracerebroventricular (i.c.v.) routes in mice.[28–30] Lower doses from 3×10^{10} gc to 5×10^{10} gc achieved widespread CNS transduction, IDS activity, and GAG reduction in the brain with normalized neurocognitive function.[28–30] These results suggest that, unlike ERT or HSCT, *in vivo* gene therapy can address CNS disease manifestations in MPS II patients.

Previously conducted MPS II clinical trials involving transduction of patient lymphocytes *ex vivo* with a retroviral vector or liver-directed gene editing did not achieve significant IDS expression.[31–33] Currently, AAV9.CB7.hIDS (RGX-121) is in clinical trials where it is administered intracisternally or i.c.v. (NCT03566043, NCT04571970) to evaluate its ability to address CNS disease manifestations. However, it is not known whether RGX-121, when administered through the CSF, is sufficient to address the peripheral and/or CNS manifestations of MPS II. In this paper, i.t. and i.v. ROAs were compared for their effectiveness and dose response in addressing both peripheral and CNS manifestations of murine MPS II as a model for genetic therapy of the human disease.

RESULTS

Study rationale and in-life evaluations

We previously reported the prevention of neurologic deficits and metabolic disease in MPS II mice after either i.v. or CSF-directed (intracerebroventricular) administration of an AAV9.CB7.hIDS vector to achieve systemic or CNS-directed expression of iduronate sulfatase.[28,34] We also observed in the i.c.v. studies that there was substantial release of AAV9.CB7.hIDS vector from the CSF, transduction of the liver, and secretion of IDS into the circulation.[28] The current study has been undertaken first of all to determine if the systemic level of enzyme achieved after AAV9.CB7.hIDS delivery through the CSF is sufficient to alleviate peripheral manifestations of disease or if supplemental i.v. administered vector is required for this purpose. Secondly, our previous i.v. and i.c.v. studies were carried out at high vector doses (5×10^{10} gc i.c.v., 1×10^{12} gc i.v.), so another goal of the current study was to determine the quantitative relationship between vector dose delivered, the level of IDS expression achieved, and associated alleviation of disease manifestations. In this study, we thus compared CNS-directed (i.t.) and systemically directed (i.v.) administration of RGX-121 (AAV9.CB7.hIDS) in a murine model of MPS II. A depiction of the AAV9.CB7.hIDS vector is shown in Figure 1A. Briefly, the vector construct consists of the constitutive CB7 promoter regulating expression of a human *IDS* sequence. Comparative effectiveness of i.t. and i.v. ROA was further evaluated by dose ranging; MPS II mice at 2 months of age were administered doses of 10^7–10^{11} gc per animal.

After vector administration, the effectiveness of gene delivery was assessed by measuring circulating levels of IDS activity (Figures 1B and 1C). Supraphysiological levels of IDS activity (150–1,300 times normal) were observed in the plasma of mice treated at the two highest doses via either ROA. For doses of 10^{10} gc and 10^{11} gc, the mean enzyme activity levels in the plasma by i.v. ROA were 5,700 nmol/h/mL and 39,400 nmol/h/mL, and by i.t. ROA they were 4,411 nmol/h/mL and 27,800 nmol/h/mL. In comparison, the average plasma enzyme activity in wild-type mice was 33 nmol/h/mL (Figures 1B and 1C; $p < 0.0001$ vs. 10^{10} gc and 10^{11} gc animals). Interestingly, animals administered 10^9 gc showed a greater than 10-fold reduction in average IDS activity over the entire time period compared to animals administered 10^{10} gc (28-fold for i.v. administered animals, $p < 0.0001$; and 93-fold for i.t. administered animals, $p < 0.0001$), with the i.v. group generating a distinctly higher average level of plasma IDS enzyme activity (176 nmol/h/mL) compared to the 10^9 gc i.t. group (47 nmol/h/mL; $p < 0.0001$). Animals dosed with 10^7 gc or 10^8 gc showed diminishingly little (i.v. administered mice) to undetectable (i.t. administered animals) levels of circulating IDS activity. In summary, doses of 10^7 gc and 10^8 gc via both ROA showed low and inconsistent levels of enzyme activity, the 10^9 gc dose demonstrated wild-type (i.t.) or just above wild-type (i.v.) enzyme activity levels, while the 10^{10} gc and 10^{11} gc doses given via either ROA showed supraphysiological levels of circulating IDS enzyme activity that were consistent over the entire study period.

Urine samples were collected over the 20-week study period to evaluate GAG excretion. Untreated MPS II controls had a demonstrably higher mean level of urine GAG over the study (2,010 μg of GAG/mg creatinine) compared to wild-type controls (775 μg of GAG/mg creatinine) ($p < 0.0001$ vs. wild type). Doses of 10^9 gc, 10^{10} gc, and 10^{11} gc given by i.v. ROA were sufficient to normalize urine GAG levels (Figure 1D) ($p < 0.0001$ vs. untreated MPS II). In comparison, only the 10^{10} gc and 10^{11} gc doses by i.t. ROA were sufficient to normalize urine GAG levels (Figure 1E) ($p < 0.0001$ vs. untreated MPS II). The 10^9 gc i.t. group exhibited normalized urine GAG (mean 793 μg GAG/mg creatinine) at the 2-week time point, but, by the end of study at 20 weeks, urine GAG in this group had increased to affected MPS II levels (mean 2,214 μg GAG/mg creatinine). Animals given doses of 10^7 gc or 10^8 gc via either ROA showed elevated levels of urine GAG throughout the study period. Overall, a minimal dose of

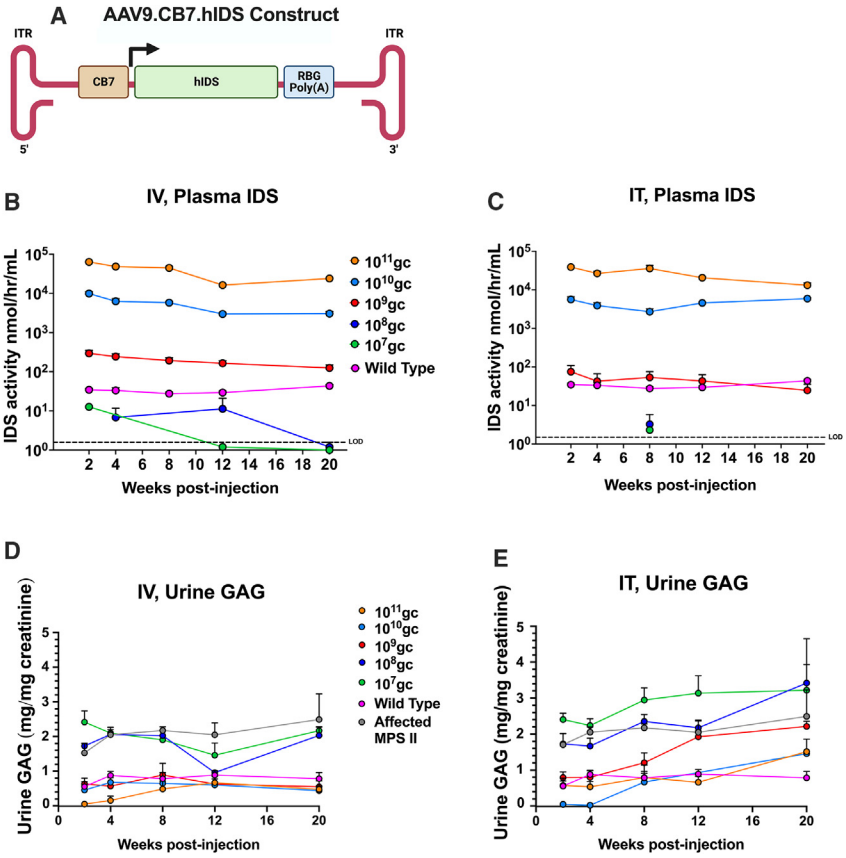

Figure 1. AAV9.CB7.hIDS vector, plasma IDS enzyme activity, and urine GAG excretion

(A) Illustration depicting the AAV9 vector. CB7, CMV immediate early enhancer with chicken β-actin promotor, exon 1 and intron 1 with rabbit beta globin splice acceptor; hIDS, human iduronate-2-sulfatase; RBG poly(A), rabbit beta globin polyadenylation sequence; ITR, AAV inverted terminal repeat. Mean plasma IDS activities by dose (key) and week (abscissa) for i.v. ROA (B) and i.t. ROA (C). MPS II and some 10^7, 10^8 samples were omitted that were below our limit of detection (LOD) as determined by 4-MU IDS assay standard curve. Excreted urine GAGs by dose (key) and week (abscissa) for i.v. ROA (D) and i.t. ROA (E). n values for all groups are provided in Table S1. Welch and Brown-Forsythe version of one-way ANOVA was used for statistical analysis, followed by Dunnett's T3 multiple comparisons test. Error bars show SEM.

10^9 i.v. or 10^{10} i.t. was needed for normalization of urine GAG excretion in MPS II mice.

Tissue IDS enzyme activity and GAG levels

At 20 weeks post administration, all mice were euthanized and tissues collected to evaluate IDS enzyme activity, GAG storage, vector biodistribution, and tissue pathology as described in section "materials and methods." Wild-type mice showed a wide range of IDS enzyme activities depending on tissue type, with the brain showing the highest IDS activity at a mean of 230.5 nmol/h/mg protein down to a mean of 4.9 nmol/h/mg protein in the heart (Figures 2A and 2B). In contrast, the affected MPS II mice had no IDS activity detectable in any tissue, with a collective average background for all tissue samples of 0.22 nmol/h/mg protein ($p < 0.0001$ vs. wild type).

Mice given 10^{11} gc i.v. exhibited IDS activity levels at or exceeding wild-type levels in all peripheral tissues ($p < 0.0001$ vs. untreated MPS II). The liver showed the highest levels of IDS activity, with an average of 4,315 nmol/h/mg protein or 181× wild type ($p < 0.0001$ vs. wild type). Animals administered 10^{10} gc i.v. also showed a high level of expression in peripheral tissues, exhibiting supraphysiological levels of enzyme activity in the liver, spleen, kidney, and heart, with other tissues showing a high percentage of wild-type activity, such as 50.5% in the lung ($p < 0.07–0.0001$ vs. untreated MPS II). The 10^9 gc dose was less effective, showing supraphysiological levels of enzyme activity only in the liver ($p < 0.0001$ vs. untreated MPS II). Little to no activity was observed in any of the other peripheral tissues of animals administered 10^9 gc, similar to animals administered 10^7 gc and 10^8 gc i.v..

Tissues from i.t. administered animals showed a pattern similar to the i.v. administered animals at the 10^{11} gc and 10^{10} gc doses. Again, the highest levels of IDS activity in animals dosed 10^{11} gc were found in the liver, with an average of 10,574 nmol/h/mg protein or 443× wild-type levels ($p < 0.0001$ vs. wild type). All peripheral tissues at this dose met or exceeded wild-type levels of IDS activity except the lung, which was 87.4 nmol/h/mg protein (85.7% wild type) ($p < 0.01–0.0001$ vs. untreated MPS II). Supraphysiological levels of enzyme activity were found in the liver, spleen, kidney, and heart of animals dosed 10^{10} gc, with closer to wild-type levels found in other major organs, such as 23% wild type in the lung ($p < 0.001–0.0001$ vs. untreated MPS II). Only the liver showed an appreciable level of enzyme activity at the 10^9 gc i.t. dose ($p < 0.0001$ vs. untreated MPS II), and the 10^7 gc and 10^8 gc doses showed little to no activity in any peripheral tissue. Overall, the 10^{10} gc dose showed similar levels of IDS enzyme activity when comparing i.v. vs. i.t. ($p = 0.2502–0.8212$), with the exception of liver. Peripheral tissues from mice treated by the i.v. ROA on average had higher levels of IDS enzyme activity than the i.t. ROA at the 10^{11} gc dose, but were not significantly different from each other ($p = 0.0785–0.3163$). The liver was the only peripheral tissue to show a significant difference between ROA at 10^{10} gc ($p < 0.0001$) and 10^{11} gc ($p < 0.03$), with i.t. administration providing a higher level of IDS activity (Figures 2A and 2B).

In peripheral tissues, with the exception of the kidney at 10^{10} gc, normalization of GAG content was observed in animals dosed at 10^{10} gc or 10^{11} gc i.v. ($p = 0.2239–0.9984$ vs. wild type). Reduced

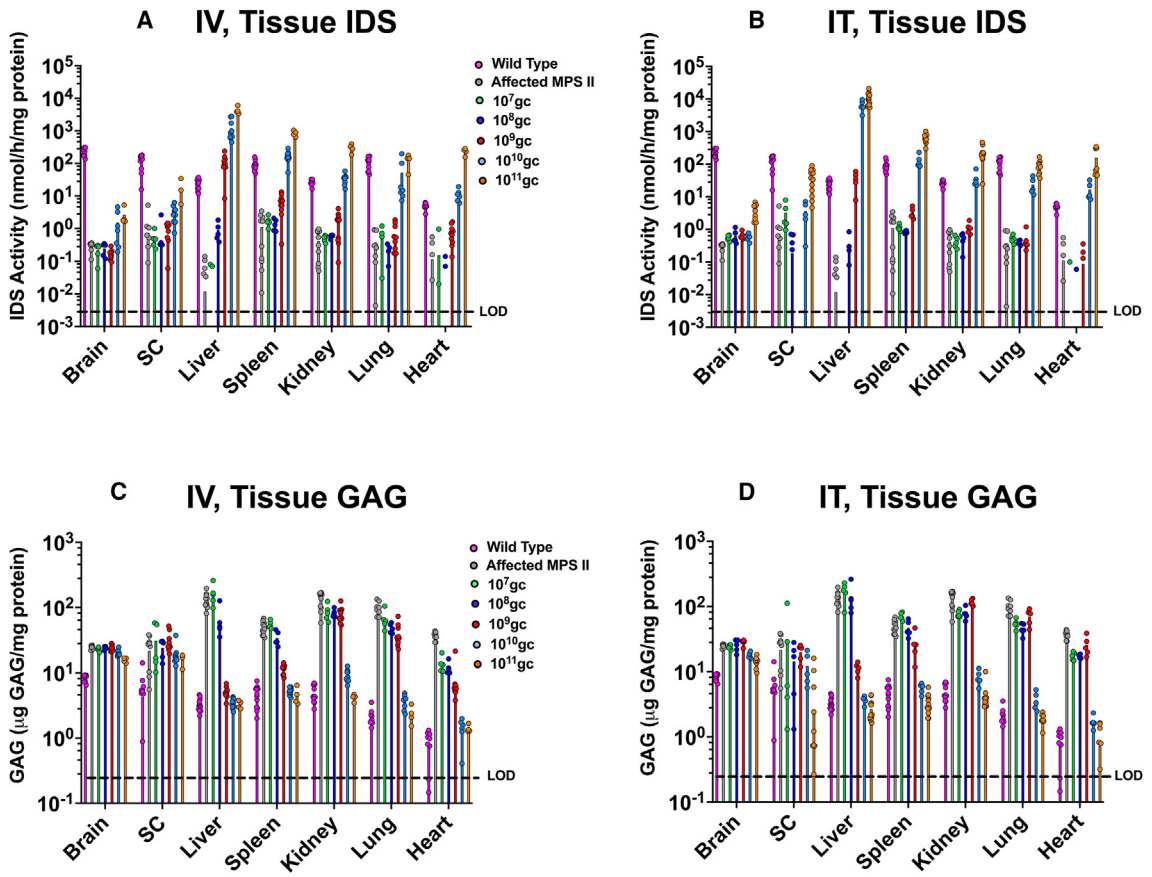

Figure 2. Tissue IDS enzyme activity and GAG levels

Individual and mean IDS activity levels by tissue and dose (key) in animals administered AAV9-hIDS by i.v. (A) or i.t. (B) ROA. Mean GAG levels by tissue and dose (key) in animals administered vector by i.v. (C) and i.t. (D) ROA. LOD (dashed line) was determined based either on IDS assay 4-MU standard curve or GAG assay glycosaminoglycan standard. Dots represent individual data points above LOD and bars the mean for that tissue/group pair. n values vary depending on tissue type and dose, as some tissues were instead taken for histologic analysis. Statistical analysis was by two-way ANOVA, followed by Tukey's multiple comparisons test.

storage material was seen at the 10^9 gc dose by i.v. ROA, notably in the liver (98.6%), spleen (84.3%), and heart (82.2%) ($p < 0.0001$–0.001 vs. untreated MPS II), but other tissues showed little to no correction in GAG content compared to affected MPS II controls (Figure 2C). By i.t. ROA, 10^{11} gc normalized GAG in all peripheral tissues ($p = 0.2404$–0.9143 vs. wild type). The 10^{10} gc administered i.t. also showed GAG normalization in most tissues as well (Figure 2D) ($p = 0.014$–0.7514 vs. wild type). The lung and kidney showed incomplete but significant reduction in GAG to 1.7× wild-type levels for both tissues (98.4% and 97.4% correction, respectively) ($p < 0.0001$ vs. untreated MPS II). Reduced GAG was seen only in the liver, spleen, and lung of animals dosed 10^9 gc i.t. ($p < 0.0001$–0.05 vs. untreated MPS II). Animals given 10^7 gc or 10^8 gc by either ROA showed little to no reduction in GAG content of any tissue. Overall, neither robust IDS enzyme activity nor significant reduction in GAG content was observed in mice treated at the 10^7 gc or 10^8 gc doses by either ROA. The 10^9 gc dose showed IDS activity comparable to wild type in the liver and GAG reductions in some but not all tissues analyzed. In contrast, at 10^{10} gc and 10^{11} gc doses, most tissues showed high if not supraphysiological levels of IDS enzyme and normalization of GAG content.

An essential part of a genetic therapy for MPS II will be to address neurologic manifestations of the disease. In this study, we examined the IDS activity levels of whole brain and spinal cord. A high level of mean IDS activity was assessed in wild-type controls, 230.5 nmol/h/mg protein in the brain and 126.2 nmol/h/mg protein in the spinal cord. Test animals exhibited average IDS activities of 3.8 nmol/h/mg protein in the brain ($p < 0.001$ vs. untreated MPS II) and 38.4 nmol/h/mg protein in the spinal cord ($p < 0.001$ vs. untreated MPS II) when administered 10^{11} gc i.t. (Figure 2B). MPS II mice administered a dose of 10^{11} gc i.v. exhibited an average of 2.6 nmol/h/mg protein in the brain ($p < 0.01$ vs. untreated MPS II) and 18.2 nmol/h/mg protein in the spinal cord ($p < 0.001$ vs. untreated MPS II) (Figure 2A). All other doses by either ROA showed <2 nmol/h/mg protein in the brain and <4 nmol/h/mg protein in the spinal cord. Although these levels of IDS activity measured in the brains of treated mice are comparatively low even at the highest

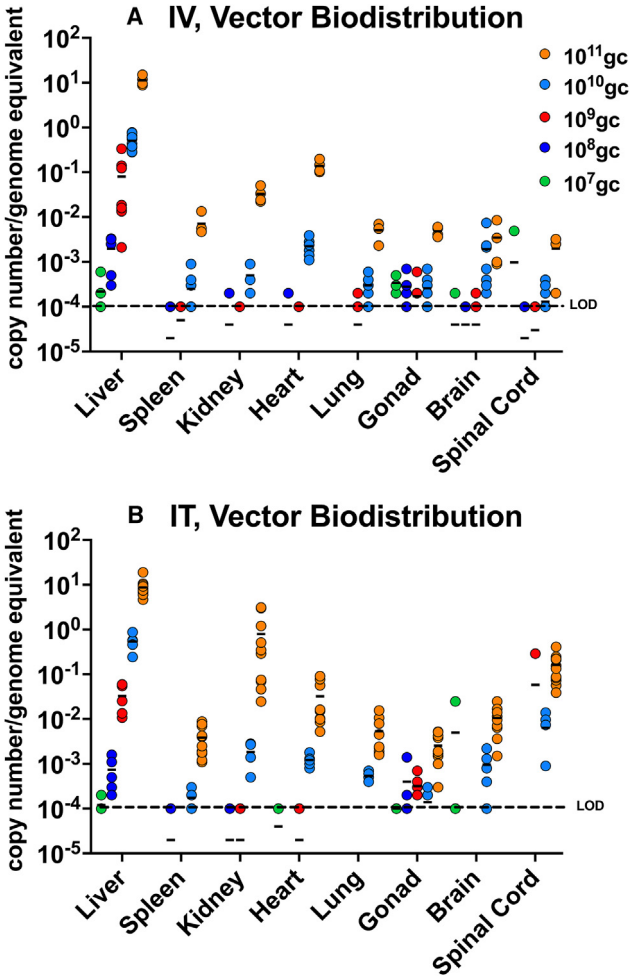

Figure 3. Vector tissue biodistribution

Vector biodistribution was determined by qPCR analysis. Results are shown for each dose (key) and indicated tissues from animals given vector by i.v. ROA (A) and i.t. ROA (B). LOD (dashed line) was determined by plasmid-based standard curve. n values vary depending on dose and tissue type as some tissues were instead taken for histologic analysis. Dots represent individual data points and horizontal lines show medians by group for each tissue. Statistical analysis was by two-way ANOVA, followed by Tukey's multiple comparisons test.

dose of 10^{11} gc i.t. (1.65% wild-type levels), previous reports have shown that <5% of wild-type activity was sufficient to normalize GAG content in the brain and ~1.5% was needed for significant reduction and prevention of neurocognitive deficits in MPS II mice.[26,35] The same tissue lysates were also extracted for GAG analysis. MPS II controls had mean GAG content that was 4.8× that of wild-type controls in the spinal cord ($p < 0.05$). The 10^{10} gc/10^{11} gc doses showed an average GAG correction of 15.6%/34.6% by i.v. administration and 55.8%/100% by i.t. administration, respectively, in the spinal cord ($p = 0.7089/0.5732$ and $0.2343/.0019$ vs. untreated MPS II). Affected MPS II controls showed mean brain GAG levels 3× that of wild-type controls ($p < 0.05$). GAG content after 10^{10} gc/10^{11} gc i.v. administration was reduced by 26.9% and 55.9% in the brain, while MPS II mice administered these vector doses by i.t. ROA showed a higher level of correction in the brain, 55.8% and 64.9%, respectively ($p = 0.5880/0.3425$ and $0.4131/0.1328$ vs. untreated MPS II) (Figures 2C and 2D). In summary, higher doses of 10^{10} or 10^{11} gc AAV-IDS vector administered via either i.v. or i.t. ROA were required to achieve detectable reduction of GAG in the CNS.

Tissue biodistribution by qPCR

Peripheral and CNS tissues were extracted for genomic DNA and assayed for vector biodistribution by qPCR for the human IDS-encoding sequence. All tissues were observed to have detectable vector copies in animals administered AAV9-IDS vector by either i.v. or i.t. ROA at 10^{10} gc and 10^{11} gc doses, with the 10^{11} gc dose on average showing more copies than the 10^{10} gc dose. The 10^{7} gc, 10^{8} gc, and 10^{9} gc doses showed few to no detectable vector copies, with the exception of liver (Figures 3A and 3B). For any dose, the vast majority of vector copies were found in the liver of both i.v. and i.t. administered animals, with the 10^{11} gc dose demonstrating the highest copy number per genome equivalent (ge) of 11.3 gc/ge and 8.8 gc/ge, respectively. These data suggest that the liver was producing a large fraction of the circulating IDS enzyme available for metabolic cross-correction in these animals. Although i.t. injection is a CNS-directed ROA, it was found to result in "global" biodistribution, transducing cells systemically as well as in the CNS, which is consistent with previous reports on CNS-directed AAV delivery (Figure 3B).[28–30] At the two higher doses of 10^{10} gc and 10^{11} gc, the i.t. ROA showed a notably higher vector distribution to the spinal cord (0.0064 gc/ge and 0.1612 gc/ge) than the i.v. ROA (0.0001 gc/ge and 0.002 gc/ge) ($p < 0.01$ and 0.05). This result is unsurprising given proximity of the spinal cord to the i.t. site of injection. In the brains of 10^{11} gc dosed mice, i.t. injection delivered more copies on average compared to i.v. injection (0.011 gc/ge vs. 0.0035 gc/ge; $p < 0.05$). Conversely, animals administered 10^{10} gc i.t. had fewer vector copies than i.v. administered animals (0.001 gc/ge vs. 0.0019 gc/ge), although this difference is not statistically significant ($p = 0.3864$).

Zygomatic arch normalization by i.t. and i.v. ROA

This MPS II mouse model exhibits a variety of skeletal manifestations, including a thickening of the zygomatic arch diameter.[36] Each dose and ROA combination was evaluated for its impact on skeletal manifestations by computed tomography at 16 weeks post administration to measure the thickness of the zygomatic arch. Affected MPS II controls had an average increase of 34.6% in zygomatic arch diameter compared to unaffected littermate controls ($p < 0.0001$). Notably, MPS II animals dosed i.v. with 10^{10} gc or 10^{11} gc showed significant decreases in zygomatic arch diameter compared to untreated MPS II controls ($p < 0.0001$ and 0.01) and were indistinguishable from wild-type controls ($p = 0.9614$ and 0.1225). The 10^{9} gc group also had significantly decreased zygomatic arch diameter ($p < 0.01$), about 50% reduced compared to affected MPS II controls (Figure 4A). Remarkably, i.t. administration of RGX-121 at doses of 10^{10} gc and 10^{11} gc into the CSF resulted in systemic delivery that was sufficient to normalize zygomatic arch diameter in MPS II mice ($p < 0.001$ and 0.0001). Animals administered the 10^{9} gc dose i.t. were not

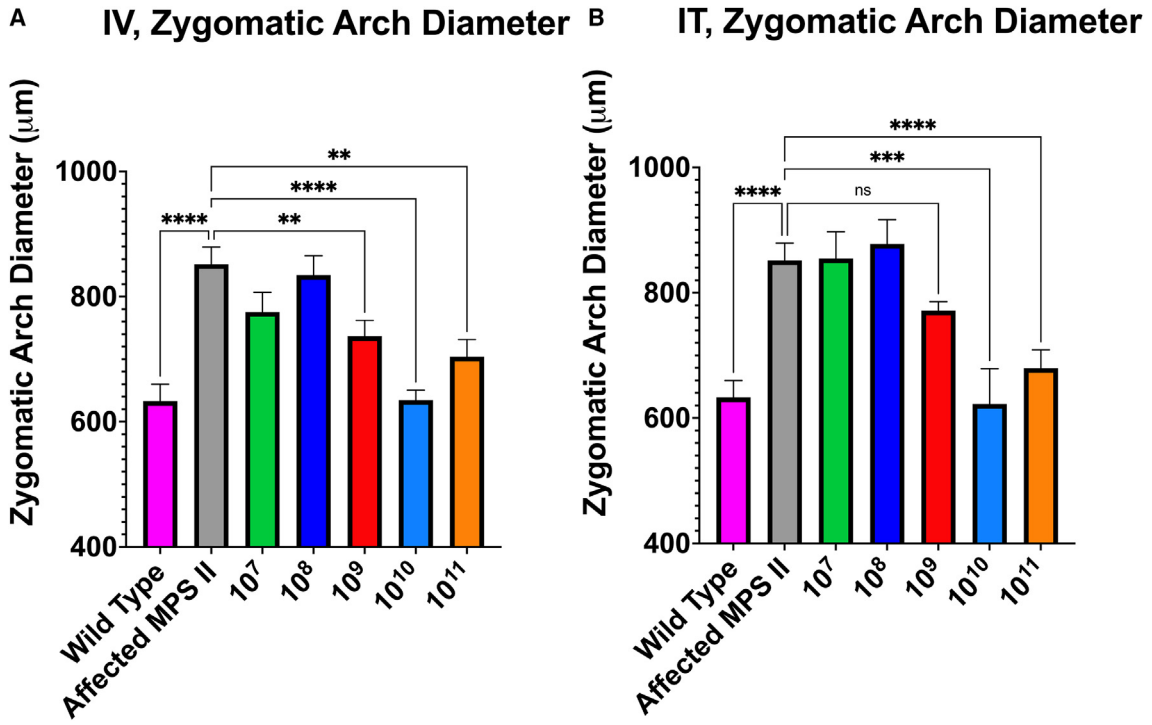

Figure 4. Zygomatic arch analysis

Zygomatic arch diameter measurements were determined by Micro-CT analysis of animals administered the indicated dose of vector by i.v. ROA (A) and by i.t. ROA (B). Significance was determined by one-way ANOVA. Sample sizes: wild type, n = 12; affected MPS II, n = 11; i.v. 10^7, 10^8, n = 5; i.v. 10^9, 10^{10}, n = 10; i.v. 10^{11}, n = 4; i.t. 10^7, 10^8, 10^9, n = 5; i.t. 10^{10}, n = 3; i.t. 10^{11}, n = 11. Error bars show SEM. ns, no significance; **p < .01, ***p < .001, ****p < .0001.

significantly different from untreated MPS II controls (Figure 4B). Animals given doses of 10^7 gc or 10^8 gc by either ROA showed no decrease in thickness of the zygomatic arch. In summary, doses of 10^{10} gc and 10^{11} gc normalized zygomatic arch diameter in MPS II mice when delivered by either ROA, while a dose of 10^9 gc partially reduced zygomatic arch diameter and only when delivered i.v.

Histological analysis

Histologic analyses were carried out in animals administered 10^{10} gc AAV9-IDS vector i.v. as this had emerged as the minimal effective dose for prevention of metabolic and skeletal disease in the MPS II mice. As a higher dose was required to achieve reduced GAG storage in the brain, histologic analysis was also carried out in animals administered 10^{11} gc i.t. Tissue samples were taken for hematoxylin and eosin (H&E) and Alcian blue (AB) staining, as well as immunohistochemistry (IHC) for lysosomal associated membrane protein-1 (LAMP-1). In contrast to wild-type mice, widespread intraneuronal vacuolization in Purkinje cells was noted in the cerebellum of MPS II mice by H&E staining (Figures 5A and 5B). H&E staining also revealed a decrease in intracellular vacuolization of Purkinje cells neurons in cerebellum for the 10^{10} gc i.v. and 10^{11} gc i.t. groups (Figures 5C and 5D). Liver H&E staining of MPS II mice showed large amounts of vacuolization in the cytoplasm of apparent resident macrophages (foam cells) but not in wild-type mice (Figures 5E and 5F). In the 10^{10} gc i.v. and 10^{11} gc i.t. groups, this vacuolization is absent in both the hepatocytes and apparent macrophages (Figures 5G and 5H). When compared to wild type, rarefaction of the smooth muscle and vacuolated macrophages were found within the tunica media in aortas of MPS II mice (Figures 5I and 5J). While the smooth muscle rarefaction was noted the 10^{10} gc i.v. and 10^{11} gc i.t. groups, vacuolated macrophages were not observed in the aorta (Figures 5K and 5L). AB staining revealed blue-positive material in the Purkinje and glial cells in MPS II but not in the wild-type group (Figures 6A and 6B). The 10^{10} gc i.v. and 10^{11} gc i.t. groups showed blue-stained material but to a lesser degree than MPS II mice (Figures 6C and 6D). While the MPS II group had AB-positive staining in liver foam cells, this was not observed in the other three groups (Figures 6E–6H). No differences in AB staining were observed in the aorta between the four groups (Figures 6I and 6L). LAMP-1 is upregulated in the cells of both MPS II mice and MPS II patients and is considered a marker of disease pathology.[37] LAMP-1 IHC staining of the cerebellum was mild in the wild-type group, but marked staining in the Purkinje and glial cells was seen in the MPS II group (Figures 7A and 7B). The 10^{10} gc i.v. and 10^{11} gc i.t. groups showed decreased staining in the Purkinje cells, but there was persistent staining in what are presumed to be glial cells (Figures 7C and 7D). In contrast to the wild-type group, the MPS II mice had widespread LAMP-1 staining in hepatocytes and foam cells (Figures 7E and 7F). A lesser degree of LAMP-1 staining was observed in the 10^{10} gc i.v. group, but 10^{11} gc i.t. mice exhibited a high amount of staining

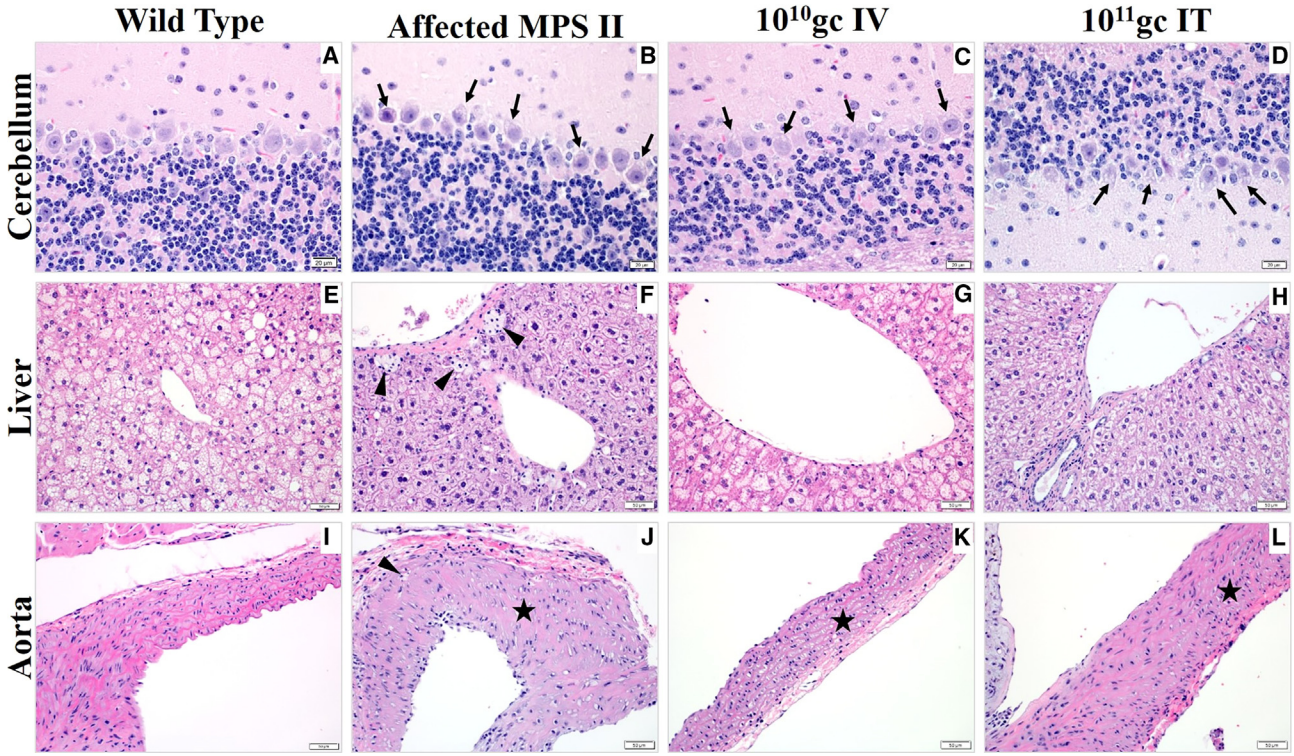

Figure 5. H&E-stained sections from 10^{10} gc i.v. and 10^{11} gc i.t. mice

(A–D) Cerebellar cortex. In contrast to the wild-type mice (A), intracytoplasmic vacuolization (black arrows) was noted in the Purkinje cells from the affected MPS II mice (B). Persistent but lesser intracytoplasmic vacuolization noted in the Purkinje cells from the 10^{10} gc i.v. (C) and 10^{11} gc i.t. (D) mice. (E–H) Liver. In contrast to the wild-type mice (E), numerous fine-vacuolated perivascular macrophages ("foam cells," black arrowheads) were seen in the affected MPS II mice (F). Foam cells were not observed in the 10^{10} gc i.v. (G) and 10^{11} gc i.t. (H) mice. (I–L) Aorta. In contrast to the wild-type mice (I), there was extensive rarefaction of the smooth muscle (black star) and few finely vacuolated macrophages (black arrowheads) within the tunica media of the affected MPS II mice (J). A similar magnitude of rarefaction was noted in the 10^{10} gc i.v. (K) and 10^{11} gc i.t. (L) mice. Scale bars, 20 μm (lower right of each micrograph).

similar to the MPS II group (Figures 7G and 7H) even though supranormal levels of IDS and normalized GAG were observed in all of these tissues. All MPS II groups (treated and untreated) showed a marked increase in LAMP-1 staining in the aorta when compared to the wild-type group (Figures 7J–7L).

Prevention of neurocognitive deficits in the Barnes maze

Mice underwent neurobehavioral testing at 4 months post administration using the Barnes maze to evaluate neurocognitive function, as described in section "materials and methods." All animals were given four trials a day over a period of 4 days, assessing the time to escape for each trial. On day one, all mice displayed some initial skill at learning the maze over the four trials, but there were no significant differences in the latency to escape between groups. For all groups, the latency to escape the maze decreased over the next 3 days as the animals learned the attendant task (Figures 8A and 8B). By day four the affected MPS II controls took significantly longer (79 s) at escaping the maze compared to wild-type controls (29 s) ($p < 0.0001$). The 10^{11} gc i.t. group was significantly faster at learning to escape the maze by day four with a mean latency to escape of 28 s ($p < 0.0002$) (Figure 8C). The 10^{11} gc i.v. group on day four also learned to escape significantly faster (20 s) compared to MPS II controls ($p < 0.0018$). The 10^{9} gc i.t. group also performed significantly faster than untreated controls ($p < 0.05$), but the 10^{10} gc i.t. group did not show significantly improved performance (perhaps due to a low N = 3 group size), suggesting that a dose of 10^{11} gc was required to prevent the emergence of neurocognitive dysfunction. All other dose and route combinations showed no significant difference when compared to MPS II affected controls. Neurocognitive decline was thus prevented in MPS II mice administered 10^{11} gc AAV9.CB7.hIDS vector by either i.t. or i.v. ROA, although more significantly for animals treated i.t.

DISCUSSION

In this study, we compared i.v. and i.t. routes of vector administration to determine if i.t. delivery alone can remedy both CNS and systemic disease manifestations. A broad range of AAV9.CB7.hIDS doses was tested to determine effectiveness in a murine model of MPS II. Mice administered vector by either i.v. or i.t. ROA at a dose of 10^{9} gc had circulating levels of IDS activity at or above wild type. However, this

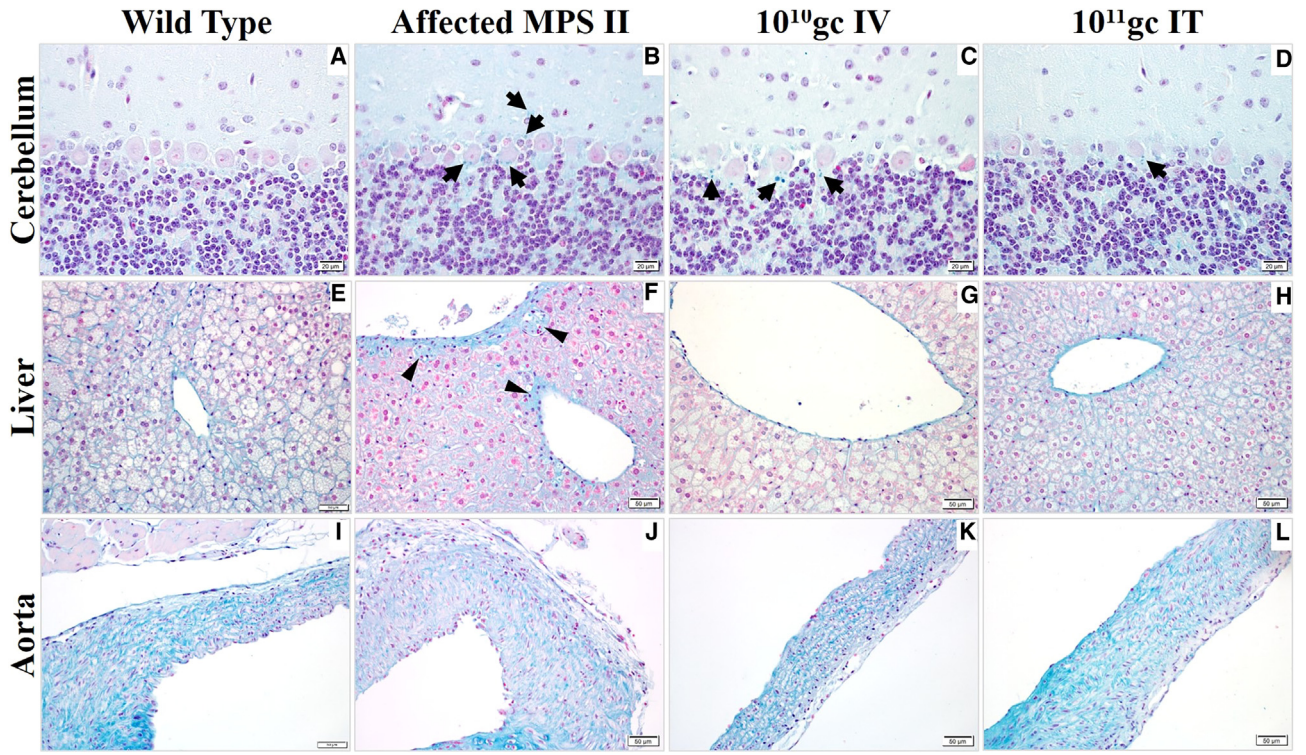

Figure 6. AB-stained sections from 10^{10} gc i.v. and 10^{11} gc i.t. mice

(A–D) Cerebellar cortex. In contrast to the wild-type mice (A), intracytoplasmic AB-positive blue material (black arrows) was noted in the Purkinje cells and presumed glia from the affected MPS II mice (B). Persistent but lesser amounts of material were noted in the Purkinje cells from the 10^{10} gc i.v. (C) and 10^{11} gc i.t. (D) mice. (E–H) Liver. In contrast to the wild-type mice (E), small amounts of AB-positive blue material (black arrowheads) were seen in presumed foam cells in the affected MPS II mice (F). No such material was observed in the 10^{10} gc i.v. (G) and 10^{11} gc i.t. (H) mice. (I–L) Aorta. No significant differences were noted in the AB-stained aortic tissues from the four groups of mice. Scale bars, 20 μm (lower right of each micrograph).

dose was insufficient to achieve wild-type levels of IDS activity and normalize GAG levels in most tissues analyzed. Mice dosed at 10^{10} gc and 10^{11} gc by either ROA exhibited circulating levels of IDS activity several logs higher than wild type, and nearly all tissues assayed met or exceeded wild-type levels of IDS activity and normalized GAG storage. While a dose of 10^{10} gc by either i.t. or i.v. ROA was sufficient to normalize zygomatic arch diameter, a higher dose of 10^{11} gc administered i.t. showed the highest level of IDS activity in the brain and the greatest reduction in GAG content, and prevented the emergence of neurocognitive deficits in the Barnes maze.

Based on the level of IDS activity achieved in the peripheral blood, a substantial amount of i.t. administered vector is released into the circulation. At a 10^{9} gc dose, levels of circulating IDS activity achieved by i.t. vector administration were 27% that of i.v. administration (Figures 1B and 1C). This is also reflected in vector biodistribution analysis of the liver, where a 10^{9} gc dose by i.t. exhibited 31% of the vector copies seen by i.v. administration (Figures 3A and 3B). The consequence of this is seen in the urine GAG excretion and zygomatic arch data, where a dose of 10^{9} gc i.v., but not i.t., was sufficient for normalization (Figures 1D, 1E, 4A, and 4B). The substantial release of vector from the CSF into the circulation and transduction of the liver with subsequent expression and secretion of IDS into the circulation is most likely the mechanism whereby i.t. administration of vector at doses of 10^{10} gc or 10^{11} gc achieves effective remedy of metabolic (i.e., GAG reduction) and skeletal (reduced zygomatic arch diameter) manifestations in the periphery of MPS II mice.

Our dose ranging revealed a pharmacodynamic threshold in the level of transduction and circulating IDS activity that was achieved when comparing lower to higher doses. The lowest doses administered, 10^{7} gc and 10^{8} gc, showed little enzyme activity, no GAG reduction, and few to no detectable copies in the tissues analyzed. AAV vector doses near this range were also recently reported to be biochemically ineffective in a mouse model of Pompe disease.[38] Quantifiable circulating IDS activity was not observed until the dose was increased from 10^{7} gc or 10^{8} gc up to 10^{9} gc. This threshold effect was also reflected in the liver biodistribution data, which comprised the majority of vector copies for any dose by either ROA. Vector copies were detectable in only a few samples at doses of 10^{7} gc and 10^{8} gc (mean $< 10^{-3}$ gc/ge) but reached a mean of nearly 0.1 gc/ge in animals dosed with 10^{9} gc (mean 40× for i.v., 44× for i.t.). Thus, 10^{9} gc was the threshold dose for either ROA. Increasing the vector dose by 10-fold from 10^{9} gc to 10^{10} gc resulted in a greater than 10-fold

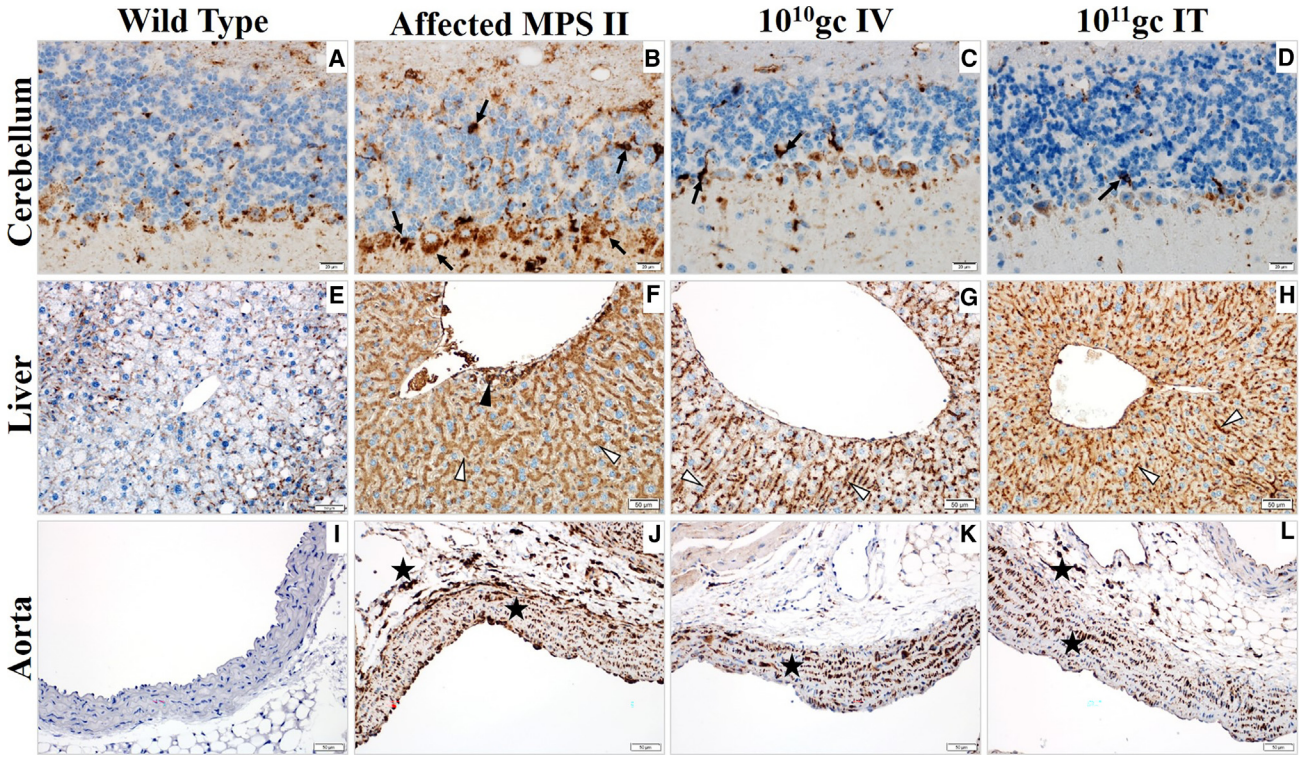

Figure 7. LAMP-1 immunostained sections from 10^{10} gc i.v. and 10^{11} gc i.t. mice

(A–D) Cerebellar cortex. In contrast to the mild intracytoplasmic LAMP1 staining in the Purkinje cells and small glia from the wild-type mice (A), there was marked intracytoplasmic LAMP1 staining (black arrows) in the Purkinje cells and presumed glia from the affected MPS II mice (B). In both the 10^{10} gc i.v. and 10^{11} gc i.t. mice, lesser amounts of LAMP1 staining was observed in the Purkinje cells, but there was persistent heavy staining within presumed glia (black arrows, C and D). (E–H) Liver. In contrast to the minimal LAMP1 staining in the liver from the wild-type mice (E), there was marked LAMP1 staining in the perivascular macrophages (black arrowheads) and hepatocytes (white arrowheads) in all the affected MPS II (F). There was lesser LAMP1 staining in the hepatocytes from the 10^{10} gc i.v. mice (white arrowhead, G) but a similarly high amount of staining in the hepatocytes from the 10^{11} gc i.t. mice (white arrowhead, H). (I–L) Aorta. In contrast to the scant LAMP1 staining in the wild-type mice (I), there was marked LAMP1 staining within the smooth muscle and macrophages (black stars) from the affected MPS II and 10^{10} gc i.v. and 10^{11} gc i.t. mice (J–L). Scale bar, 20 μm (lower right of each micrograph).

increase in circulating IDS activity levels for both i.v. (28-fold) and i.t. (93-fold) administered animals, indicating that the lower dose threshold had been overcome. The increase in IDS activity levels after i.t. administration was 3.3× that of i.v. administration. When the vector dose was increased from 10^{10} gc to 10^{11} gc, i.t. and i.v. administered animals showed a similar 6.3-fold and 6.9-fold increase in plasma activity levels, respectively (i.v. 1.1× increase over i.t.) (Figures 1B and 1C), i.e., less than a dose-consistent 10-fold. Thus, vector administered at higher doses approached a steady state in which vector distribution and transduction were much less affected by the lower dose threshold and may in fact give way to a saturation effect.

One possible explanation for the threshold effect is the existence of pre-existing anti-AAV antibodies. Under these conditions, antibody-mediated neutralization may interrupt *in vivo* transduction at lower vector doses.[39] Previous studies in both mice and non-human primates have demonstrated that neutralizing antibodies can reduce or completely block AAV vector transduction in the liver.[40–42] Other mechanisms of vector neutralization include innate immune responses such as activation of toll-like receptors or complement-induced macrophage-mediated destruction of the vector in the liver.[43,44] Our data showing a reduced threshold impact as the dose is increased from 10^9 gc to 10^{11} gc (in which a smaller percentage of the overall dose is neutralized by the threshold effect) is consistent with such an antibody or cellular mechanism.

Decreasing plasma IDS activity over time was seen in animals given doses of 10^9 gc, 10^{10} gc, or 10^{11} gc via either i.t. or i.v. ROA. With the exception of 10^{10} gc i.t., the circulating IDS activity at week 20 was approximately one-third that of their respective 2-week time point (Figures 1B and 1C). As previously reported by this and other laboratories,[27,28,45–47] much of the circulating enzyme is expressed in the liver, given the vast majority of vector copies found there. Loss of transduced hepatocytes could be one cause for the observed decline in circulating IDS activity over time. It is unlikely that this was due to natural hepatocyte turnover, which takes 200–400 days in mice,[48] much greater than the 20-week study period. Reduced IDS activity over time could also be due to a cellular or humoral

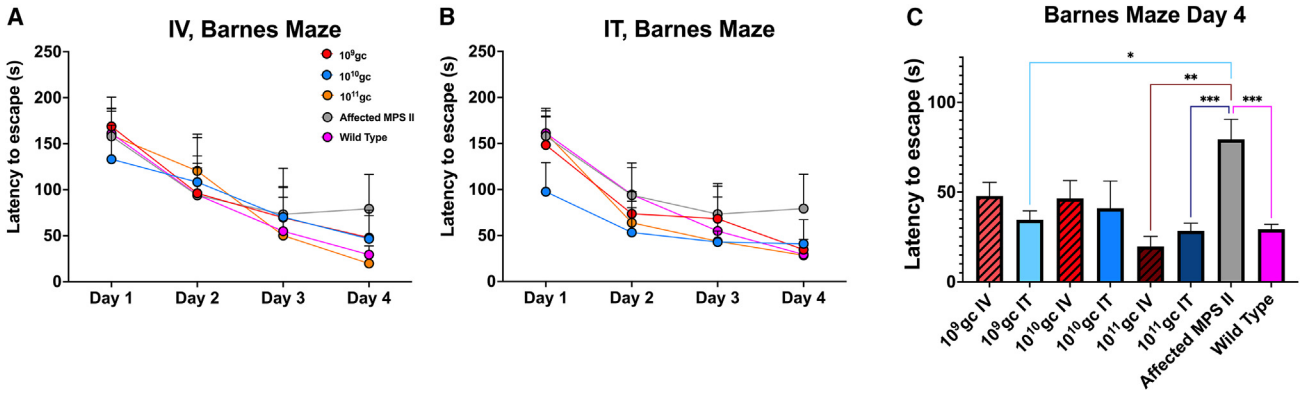

Figure 8. Neurocognitive analysis by Barnes maze

All groups underwent neurobehavioral testing at 6 months of age. Barnes maze evaluation for long-term spatial learning and memory in i.v. (A) and i.t. (B) mice. Results are shown as the mean latency to escape of four trials per day over 4 days. (C) All Significant differences between groups were observed on day four of testing. Significance was determined by two-way ANOVA. Sample sizes are wild type, n = 12; affected MPS II, n = 11; i.v. 10^9 gc, n = 10; i.v. 10^{10} gc, n = 10; i.v. 10^{11} gc, n = 4; i.t. 10^9 gc, n = 5; i.t. 10^{10} gc, n = 3; i.t. 10^{11} gc, n = 11. Error bars shown are mean ± SD. ***p < 0.001.

anti-IDS immune response[49,50]; however, such a response would be expected to shut down IDS in tissues and in the circulation, and we have not seen evidence for such a response in any of our MPS II studies to date.[28,34,35] The observed effect was not entirely consistent, as the IDS level in any given month was not always lower than the preceding month, and loss of IDS activity over time was not observed in the aforementioned 10^{10} gc i.t. group. With the exception of 10^9 gc i.t., the decreasing plasma levels over time were not associated with a reciprocal rise in urine GAG excretion (Figures 1B–1E). Thus, for our higher doses there was no decreased effectiveness in GAG reduction over time. Additionally, other studies have shown that AAV-mediated gene expression can persist in mice for at least a year,[20,51] and AAV-mediated gene expression in dogs and humans has been reported to persist for at least several years.[51–53]

An integral part of next-generation therapy for MPS II will be to address neurological manifestations of the disease that affects approximately two-thirds of patients.[1] Animals administered 10^{11} gc i.t. had the highest levels of IDS activity in the CNS, and the level of activity in the spinal cord at this dose was 30% of the wild-type level, sufficient to normalize GAG content. In wild-type mice, IDS activity was highest in the brain compared to any other tissue analyzed, similar to past studies.[27,28,30] Thus, the level of IDS activity achieved in mice administered 10^{11} gc i.t. corresponded to only a small fraction (1.65%) of wild-type activity (Figure 2B). However, previous studies have shown that as little as 1.5% of wild-type activity is sufficient for meaningful reduction of GAG content in the brain that prevents emergence of neurocognitive deficits in MPS II mice.[26,35,54] Indeed, mice treated at a dose of 10^{11} gc i.t. demonstrated mean correction of 65% in brain GAG content (Figure 2D). In addition, this group showed a decrease in cerebellar Purkinje cell vacuolization, AB-positive material, and LAMP-1 staining, as well as prevention of neurocognitive deficits as measured in the Barnes maze (Figures 5A–5D and 8C). The same dose delivered i.v. also showed improved biochemical and neurobehavioral outcomes.

What it is that limits the level of IDS activity in the brain after AAV-mediated transduction has yet to be determined. Even i.c.v. administration of AAV9.CB7.hIDS vector at high dose (5×10^{10}) resulted in only 40% of the endogenous level of IDS.[28–30] By comparison, our companion study on MPS I showed that, in MPS I mice, a dose of 10^{10} gc AAV9.CB7.hIDUA administered either i.v. or i.t. produced enzyme levels in the brain that were 10- to 20-fold higher than wild type, with the i.t. group achieving a mean level of ∼100 nmol/h/mg protein (L.R. Belur et al., unpublished data). Further investigation is needed to determine why, given an otherwise identical vector construction and ROA, AAV9.CB7.hIDS performs less effectively in MPS II mice compared to AAV9.CB7.hIDUA in MPS I mice.

The brains of MPS II mice treated at higher doses (10^{10} or 10^{11} gc) by either ROA showed between 26.9% and 64.9% GAG correction and, with the exception of 10^{10} gc i.t., detectable IDS activity. IDS activity in the brain could be derived from enzyme that was generated either inside or outside of the CNS. AAV9 has been shown to cross the BBB,[55] and vector copies were detected in the CNS, suggesting transduction and IDS expression in the brain. Indeed, mice administered AAV9.CB7.hIDS vector i.t. had higher vector copies in the brain than mice equivalently dosed i.v., suggesting a higher level of CNS transduction via this ROA. However, we cannot rule out transduction that is limited to the vasculature by either ROA as previously reported in i.v. studies.[34,56–58] Another possibility is the so called high-dose effect that has been reported in preclinical gene therapy studies for MPS I and MPS II, whereby a small fraction of sufficiently high-level circulating enzyme enters the CNS from the blood.[26,35,56] IDS detected in the brain could also have been derived from a combination of vector transduction in the tissue plus transit of enzyme from the circulation. In this case, i.t. administered vector transduces cells in the CNS that secrete enzyme available for cross-correction. At the same time, a

portion of the administered vector is released into the circulation and transduces the liver to provide a robust and consistent level of circulating IDS enzyme that can exert the high-dose effect and transit into the CNS. Additional study is warranted to further characterize the source of enzyme in the CNS after CSF-directed as well as systemic AAV vector administration.

We found that mice administered AAV9.hIDS by either ROA at a dose of 10^{10} gc or 10^{11} gc showed normalization of skeletal disease as exemplified by zygomatic arch diameter. This is consistent with previous MPS I and MPS II gene therapy studies.[54,59–61] A lentiviral vector-based approach to MPS II was used to investigate skeletal complications in-depth and found that a high level of IDS in the serum reduced GAGs and normalized bone metabolism, leading to bone remodeling in the zygomatic arch.[60] The *in vivo* AAV9-based approach reported here likely mediates zygomatic arch normalization through the same mechanism, given the high and consistent levels of circulating enzyme assessed in animals administered 10^{10} gc or 10^{11} gc.

Comparing i.v. and i.t. ROAs in the context of a dose-ranging study provided considerable insight into effective dosing for treatment of MPS II in a murine model of the disease. This study finds that a dose of 10^{11} gc, i.v. or i.t., was able to address both CNS and systemic disease manifestations. A dose of 10^{10} gc administered either i.v. or i.t. was minimally sufficient to normalize peripheral manifestations (tissue GAG and zygomatic arch diameter). Similar dose effectiveness has been reported in studies evaluating i.c.v. injection of 3×10^{10} gc[41] or 5×10^{10} gc AAV9.CB7.hIDS vector.[28] These slightly lower doses are similar to our optimal dose of 10^{11} gc, as in our hands i.c.v. infusion achieves about a 10-fold higher level of transduction than i.t. infusion.[62] i.v. administration of AAV9-IDS has been previously tested at doses ranging from 2.5×10^{11} gc up to 2×10^{13} gc.[27,34,35] In contrast, we found that as little as 10^{10} gc (5×10^{11} gc/kg) AAV9.CB7.hIDS administered i.v. normalized GAG in peripheral tissues and prevented emergence of a key skeletal manifestation. In clinical trials employing AAV vector, a wide range of total doses have been administered, from 5.8×10^{9} gc to 7.5×10^{15} gc for targeted delivery and 3.5×10^{13} gc to 1.5×10^{17} gc for systemic delivery.[63] AAV-based gene therapies have encountered issues with safety, such as those that emerged in a clinical trial of X-linked myotubular myopathy,[64,65] and efficacy, as seen in clinical trials of AAV in the treatment of hemophilia[49,66,67] related to the dose of vector that is administered. Studies evaluating outcomes to determine safe and effective preclinical dosing are thus essential for clinical trial design and translation of AAV-based gene therapies.

By comparing i.v. vs. i.t. AAV9.CB7.hIDS administration at varying doses, this study highlights the use of CNS-directed vector delivery to address both neurologic and systemic disease manifestations in a murine model of MPS II. The substantial release of vector into the periphery after CSF-mediated delivery of AAV9 suggests that this approach could be evaluated in the treatment of other disorders that exhibit both CNS and systemic manifestations, such as MPS I, MPS VII, Gaucher disease, and Danon disease.[68–70] Investigating these ROAs in a dose-ranging format determined the minimal dosing for both CNS and peripheral manifestations (10^{11} gc) as well as for peripheral manifestations alone (10^{10} gc). The value of such a dose-ranging study is in identifying a therapeutically efficacious dose while minimizing toxicities associated with high dosing. Our work here suggests that non-neuronal MPS II can be treated either through a low systemic dose or by redistribution from the CSF following i.t. dosing when targeting CNS manifestations of MPS II disease. The value of this approach over ERT is that, rather than the low, inconsistent levels of IDS provided from frequent infusions of enzyme, a one-time i.v. administration of AAV9.CB7.hIDS showed consistent and high levels of systemic IDS.[6] In addition, ERT at currently administered doses does not remedy the CNS manifestations of neuronopathic MPS II. It is thus critical that the next generation of therapies for MPS II address neurologic disease. Herein, we report that dosing 10^{11} gc with AAV9.CB7.hIDS in MPS II mice remedied CNS disease by providing IDS to the brain, reducing GAG content, and preventing the emergence of neurocognitive deficits. Overall, these results suggest the potential effectiveness of AAV9.CB7.hIDS to remedy neurologic as well as peripheral disease in MPS II patients as well.

MATERIALS AND METHODS

Animal husbandry

All animal husbandry and procedures were compliant with and approved by the University of Minnesota Institutional Animal Care and Use Committee (IACUC). Wild-type C57BL/6 mice were purchased from the National Cancer Institute or Envigo and C57BL/6 iduronate-2-sulfatase knockout (IdS-KO) mice were graciously provided by Dr. Joseph Muenzer of the University of North Carolina.[36] Offspring were genotyped by PCR and maintained at University of Minnesota Research Animal Resources facilities under specific pathogen-free conditions. Animals were provided food and water *ad libitum*.

AAV vector design and production

RGX-121 was designed, constructed, and packaged by REGENXBIO (Rockville, MD). The vector plasmid consisted of (1) the CB7 promoter sequence (chicken β-actin promoter and cytomegalovirus immediate-early enhancer) and chimeric intron (chicken β-actin intron with intron 2 splice acceptor, rabbit β-globin exon 3); (2) a *hIDS* coding sequence; (3) a rabbit B globin polyadenylation signal; and (4) AAV2 inverted terminal repeats (ITRs) flanking the IDS transcription unit. This AAV vector construct was packaged[28] by co-transfection with an AAV2/9 rep/cap plasmid along with adenovirus helper plasmid pAdDF6 into HEK293 cells. Vector product was purified from cell supernatant by affinity chromatography as previously described.[71] For potency assessment, the vector which was titered by digital droplet PCR.[71]

AAV vector administration

Genotyped MPS II mice were administered total AAV9 vector doses of 10^{7}, 10^{8}, 10^{9}, 10^{10}, or 10^{11} gc at 2 months of age. The i.v. injections were given in a 100-μL volume through the lateral tail vein. The i.t. injections were given to conscious animals in a 10-μL volume between

the L5 and L6 vertebrae as previously described.[62,72,73] Briefly, a syringe needle (30G, 0.5 inch) that had been previously removed from its plastic hub was connected to a length of PE10 tubing, which was then connected to a second needle that was attached to a 50-mL Luer-hub Hamilton syringe. The injection was delivered by gently holding the hip bones (iliac crest) of the mouse and inserting the needle (bevel side up) at about a 45° angle centered between the hip bones of the iliac crest. The experimenter positioned the needle such that it slipped between the vertebrae and made contact with the dura mater. A reflexive flick of the tail indicated penetration of the dura mater. The experimenter then depressed the Hamilton syringe and delivered the injectate into the CSF of the i.t. space.

Tissue processing

Animals were euthanized at 4 or 7 months of age by CO_2 asphyxiation and transcardially perfused with 0.9% normal saline. A necropsy was performed, and tissues (liver, spleen, kidney, brain, heart, lung, spinal cord, and gonad) were harvested, frozen on dry ice, and stored at −20°C until processed. A section of each tissue was fixed in 10% neutral buffered formalin (VWR) at a ratio of 1:10–20 v/v tissue to formalin, and, after 24–48 h, transferred to 70% ethanol for storage and histologic analysis. A Bullet Blender bead mill (Storm 24 Homogenizer, Next Advance) was used to process tissues for biochemical analysis by homogenization in 0.9% saline as previously described[28,35] and clarified by centrifugation in a 5424R Eppendorf centrifuge. The clarified supernatants were termed tissue lysates and were used for protein, IDS, and GAG assays. Unclarified homogenates were used for qPCR analysis. Homogenates and lysates were stored at −20°C until further processing or analysis.

IDS enzyme activity

IDS enzyme activity in plasma and tissue lysates was determined in a fluorometric assay using 4-methylumbelliferyl α-l-iduronide 2-sulfate disodium salt (4-MU2S) as substrate (catalog # M334715, Toronto Research Chemicals or catalog # EM03201, Carbosynth) as previously described.[35,74] Then 5 mg of 4-MU2S substrate was dissolved in 8.33 mL of substrate buffer (0.1M Na-acetate buffer, pH 5.0 + 10 mM Pb-acetate + 0.02% (w/v) Na-azide) to yield a 1.25 mM working solution. Then 10-μL aliquots of plasma or tissue lysates were mixed with 20-μL aliquots of working substrate and incubated at 37°C for 1.5 h. The IDS reaction was then stopped with the addition of 20 μL of PiCi buffer (0.2M Na_2HPO_4 + 0.1 M citric acid, 0.02% Na-azide, pH 4.5). Then 10 μL of 5 μg/mL alpha-L-iduronidase (IDUA) (catalog # 4119-GH, Bio-Techne) was added and incubated at 37°C overnight. The reaction was terminated by adding of 200 μL of stop buffer (0.5 M Na_2CO_3 + 0.5 M $NaHCO_3$, pH 10.7) and then the reaction mixture was centrifuged at ∼13,000 rpm for 1 min. The supernatant was transferred into a black 96-well round-bottom plate and the resulting fluorescence was measured using a Bio-Tek Synergy Mx plate reader with excitation at 355 nm and emission at 460 nm. A 4-MU (Sigma #M1381) standard curve was used to calculate the amount of 4-MU produced in the reaction. Tissue lysates were also assayed for total protein using Pierce protein assay reagent (catalog # 22660, Thermo Fisher). Enzyme activity is expressed as nmol 4-MU released per milligram of protein per hour (nmol/h/mg) for tissues extracts, and as nmol/h/ml for plasma. All samples were assayed in duplicate.

GAG assay

Proteinase K (20 mg/mL) was mixed with tissue lysates at a ratio of 1:10 (ProK:tissue lysate) and incubated at 55°C overnight, followed by proteinase K inactivation by boiling for 10 min. Then 50 μL of tissue lysate was then digested with 200 units of DNase and 2 mg of RNase at room temperature overnight. Nucleases were inactivated by boiling for 10 min. GAG levels were determined using the Blyscan Sulfated Glycosaminoglycan Assay kit (Biocolor Life Science Assays, Accurate Chemical, NY, catalog # CLRB1000) according to the manufacturer's instructions, with results expressed as micrograms of GAG per milligram of lysate protein. GAG levels were assayed in unprocessed urine using the Blyscan kit, normalizing to urine creatinine (creatinine levels were determined using a creatinine assay kit; Sigma, MAK080), and expressed as micrograms of GAG per milligram of creatinine.

Vector biodistribution by qPCR

Tissue homogenates were incubated with proteinase K overnight at 55°C and then genomic DNA was extracted using phenol-chloroform. For qPCR of the codon-optimized *IDS* sequence, each reaction contained 100 ng of gDNA template, 2× IQ SYBR Green Supermix (Bio-Rad), 5 pmol/μL forward primer (5′-CCCTGGTAATCCCCGT GAAC-3′), 5 pmol/μL reverse primer (5′-TGGTGCGTATGGAA TAGCCC-3′), and nuclease-free water to a volume of 25 μL. Thermocycler parameters were 95°C for 5 min, followed by 40 cycles of 95°C for 15 s, 59°C for 30 s, and 72°C for 45 s in a Bio-Rad C1000 Touch Thermo Cycler. A standard curve was generated by serial dilution of plasmid pAAV.CB7.CI.hIDS.RBG.KanR. qPCR results from analysis are expressed as vector copies per genome equivalent.

Radiographic analysis of zygomatic arch

One week before euthanasia, all experimental animals underwent micro-computed tomography (CT) imaging using a Siemens Inveon PET/CT machine. The animals were sedated with 5% isoflurane before imaging. Micro-CT imaging produced DICOM (Digital Imaging and Communications in Medicine) image files that were converted to Imaris image file format using Imaris File Converter software. The Imaris images were analyzed using Imaris 3D Analysis software.

Histopathology

Processing of formalin-fixed tissues was carried out by a graded series of alcohols. For H&E analysis, tissues were embedded in paraffin and 4-μm sections were cut and stained. For AB staining, 4-μm sections were cut, deparaffinized, and hydrated to distilled water. Sections were immersed in a solution of 3% acetic acid for 3 min and subsequently stained with AB for 30 min. After rinsing with running tap water and then distilled water, the slides were counterstained with nuclear fast red. For LAMP1 IHC, 4-μm formalin-fixed, paraffin-embedded (FFPE) sections were deparaffinized, rehydrated, and

submitted to heat-induced antigen retrieval in EDTA. Slides were incubated with a 1:500 diluted rabbit monoclonal anti-LAMP antibody (ab208943, Abcam) overnight at 4°C. Following this, the slides were incubated with Rabbit Envision (Dako) for 30 min and then chromogen 3,3′-diaminobenzidine (DAB) before hematoxylin counterstaining.

Barnes maze

The Barnes maze is a measure of spatial navigation and memory.[75] The maze is composed of a circular platform with 20 holes located around the periphery, all of which are blocked with the exception of the escape hole. The escape hole has a box placed underneath, which is accessible to the mouse. Visual cues are placed on the walls surrounding the maze, which are used by the mice for spatial navigation. The mouse is placed in the center of the maze under bright overhead lights and given 3 min to explore the maze. If the mouse does not enter the escape box within 3 min, it is gently guided to the escape hole and left there for 15–30 s before returning to its home cage. The mice were given trials on the Barnes maze four times a day for 4 days, with an interval of 10–20 min between any two consecutive trials for each mouse. The time taken by the animal to enter the escape hole was recorded as latency to escape.

Statistics

Microsoft Excel was used for calculations and analysis. GraphPad Prism was used for graphing and statistics. For plasma IDS and urine GAG activity, the Welch and Brown-Forsythe version of one-way analysis of variance (ANOVA) was used, followed by Dunnett's T3 multiple comparisons test. For tissue IDS activity, tissue GAG activity, and vector biodistribution, two-way ANOVA followed by Tukey's multiple comparisons test was used. One-way ANOVA was utilized for group comparisons in radiographic data. Multiple group comparisons were evaluated by two-way ANOVA for Barnes maze. p values of <0.05 were considered statistically significant for all tests.

DATA AND CODE AVAILABILITY

The data generated during the study are presented in this original research article and were used to draw its conclusions. Additional data, protocols, or other information can be requested by contacting the corresponding author.

SUPPLEMENTAL INFORMATION

Supplemental information can be found online at https://doi.org/10.1016/j.omtm.2024.101201.

ACKNOWLEDGMENTS

Neurobehavioral studies were conducted at the University of Minnesota Mouse Behavior Core (supported by NIH grant NS062158). The authors thank core director Dr. Lind for help and advice with testing. The authors thank Dr. Joseph Muenzer for generously supplying the IDS knockout mouse strain. M.C.S. was supported in part by grant # 5T32GM113846-10 Stem Cell Biology Training Program T32 at the University of Minnesota. This work was funded by REGENXBIO.

AUTHOR CONTRIBUTIONS

M.C.S., experimental design and coordination, tissue processing, biochemical assays (IDS activity, GAG, DNA extraction, and qPCR assays), neurobehavioral testing, data compilation and analysis, and lead role in manuscript writing; L.B., study design and data interpretation; A.D.K., animal husbandry; O.E., IDS enzyme assay, GAG assay, DNA extraction, and qPCR; J.F. and T.L., micro-CT radiography and analysis; D.S., histopathologic analysis and manuscript writing; K.F.K. and C.A.F., i.t. injections; K.H.K., coordination and manuscript writing; N.B., study design and coordination and project management. R.S.M., study design and coordination, project management, data interpretation, and manuscript writing.

DECLARATION OF INTERESTS

The work detailed in this article was sponsored by REGENXBIO. K.H.K. and N.B. are current or former employees of Regenxbio. L.R.B., T.C.L., C.A.F., N.B., and R.S.M. are coinventors on patents related to the contents of this manuscript. R.S.M. is also an employee of Immusoft.

REFERENCES

1. Hampe, C.S., Yund, B.D., Orchard, P.J., Lund, T.C., Wesley, J., and McIvor, R.S. (2021). Differences in MPS I and MPS II Disease Manifestations. Int. J. Mol. Sci. *22*, 7888. https://doi.org/10.3390/ijms22157888.

2. Neufeld, E.F., and Muenzer, J. (2019). The Mucopolysaccharidoses. In The Online Metabolic and Molecular Bases of Inherited Disease, D.L. Valle, S. Antonarakis, A. Ballabio, A.L. Beaudet, and G.A. Mitchell, eds. (McGraw-Hill Education).

3. Wraith, J.E., Scarpa, M., Beck, M., Bodamer, O.A., De Meirleir, L., Guffon, N., Meldgaard Lund, A., Malm, G., Van der Ploeg, A.T., and Zeman, J. (2008). Mucopolysaccharidosis type II (Hunter syndrome): a clinical review and recommendations for treatment in the era of enzyme replacement therapy. Eur. J. Pediatr. *167*, 267–277. https://doi.org/10.1007/s00431-007-0635-4.

4. Martin, R., Beck, M., Eng, C., Giugliani, R., Harmatz, P., Muñoz, V., and Muenzer, J. (2008). Recognition and diagnosis of mucopolysaccharidosis II (Hunter syndrome). Pediatrics *121*, e377–e386. https://doi.org/10.1542/peds.2007-1350.

5. Al Sawaf, S., Mayatepek, E., and Hoffmann, B. (2008). Neurological findings in Hunter disease: pathology and possible therapeutic effects reviewed. J. Inherit. Metab. Dis. *31*, 473–480. https://doi.org/10.1007/s10545-008-0878-x.

6. Garcia, A.R., DaCosta, J.M., Pan, J., Muenzer, J., and Lamsa, J.C. (2007). Preclinical dose ranging studies for enzyme replacement therapy with idursulfase in a knockout mouse model of MPS II. Mol. Genet. Metabol. *91*, 183–190. https://doi.org/10.1016/j.ymgme.2007.03.003.

7. Whiteman, D.A., and Kimura, A. (2017). Development of idursulfase therapy for mucopolysaccharidosis type II (Hunter syndrome): the past, the present and the future. Drug Des. Dev. Ther. *11*, 2467–2480. https://doi.org/10.2147/DDDT.S139601.

8. Muenzer, J., Gucsavas-Calikoglu, M., McCandless, S.E., Schuetz, T.J., and Kimura, A. (2007). A phase I/II clinical trial of enzyme replacement therapy in mucopolysaccharidosis II (Hunter syndrome). Mol. Genet. Metabol. *90*, 329–337. https://doi.org/10.1016/j.ymgme.2006.09.001.

9. Muenzer, J., Wraith, J.E., Beck, M., Giugliani, R., Harmatz, P., Eng, C.M., Vellodi, A., Martin, R., Ramaswami, U., Gucsavas-Calikoglu, M., et al. (2006). A phase II/III clinical study of enzyme replacement therapy with idursulfase in mucopolysaccharidosis II (Hunter syndrome). Genet. Med. *8*, 465–473. https://doi.org/10.1097/01.gim.0000232477.37660.fb.

10. Muenzer, J., Beck, M., Eng, C.M., Giugliani, R., Harmatz, P., Martin, R., Ramaswami, U., Vellodi, A., Wraith, J.E., Cleary, M., et al. (2011). Long-term, open-labeled extension study of idursulfase in the treatment of Hunter syndrome. Genet. Med. *13*, 95–101. https://doi.org/10.1097/GIM.0b013e3181fea459.

11. Parini, R., Rigoldi, M., Tedesco, L., Boffi, L., Brambilla, A., Bertoletti, S., Boncimino, A., Del Longo, A., De Lorenzo, P., Gaini, R., et al. (2015). Enzymatic replacement therapy for Hunter disease: Up to 9 years experience with 17 patients. Mol. Genet. Metab. Rep. *3*, 65–74. https://doi.org/10.1016/j.ymgmr.2015.03.011.

12. D'Avanzo, F., Rigon, L., Zanetti, A., and Tomanin, R. (2020). Mucopolysaccharidosis Type II: One Hundred Years of Research, Diagnosis, and Treatment. Int. J. Mol. Sci. *21*, 1258. https://doi.org/10.3390/ijms21041258.

13. Muenzer, J., Burton, B.K., Harmatz, P., Gutiérrez-Solana, L.G., Ruiz-Garcia, M., Jones, S.A., Guffon, N., Inbar-Feigenberg, M., Bratkovic, D., Hale, M., et al. (2022). Intrathecal idursulfase-IT in patients with neuronopathic mucopolysaccharidosis II: Results from a phase 2/3 randomized study. Mol. Genet. Metabol. *137*, 127–139. https://doi.org/10.1016/j.ymgme.2022.07.017.

14. Biffi, A. (2017). Hematopoietic Stem Cell Gene Therapy for Storage Disease: Current and New Indications. Mol. Ther. *25*, 1155–1162. https://doi.org/10.1016/j.ymthe.2017.03.025.

15. Kubaski, F., Yabe, H., Suzuki, Y., Seto, T., Hamazaki, T., Mason, R.W., Xie, L., Onsten, T.G.H., Leistner-Segal, S., Giugliani, R., et al. (2017). Hematopoietic Stem Cell Transplantation for Patients with Mucopolysaccharidosis II. Biol. Blood Marrow Transplant. *23*, 1795–1803. https://doi.org/10.1016/j.bbmt.2017.06.020.

16. Selvanathan, A., Ellaway, C., Wilson, C., Owens, P., Shaw, P.J., and Bhattacharya, K. (2018). Effectiveness of Early Hematopoietic Stem Cell Transplantation in Preventing Neurocognitive Decline in Mucopolysaccharidosis Type II: A Case Series. JIMD Rep. *41*, 81–89. https://doi.org/10.1007/8904_2018_104.

17. Horgan, C., Jones, S.A., Bigger, B.W., and Wynn, R. (2022). Current and Future Treatment of Mucopolysaccharidosis (MPS) Type II: Is Brain-Targeted Stem Cell Gene Therapy the Solution for This Devastating Disorder? Int. J. Mol. Sci. *23*, 4854. https://doi.org/10.3390/ijms23094854.

18. Sands, M.S., and Davidson, B.L. (2006). Gene therapy for lysosomal storage diseases. Mol. Ther. *13*, 839–849. https://doi.org/10.1016/j.ymthe.2006.01.006.

19. Zincarelli, C., Soltys, S., Rengo, G., and Rabinowitz, J.E. (2008). Analysis of AAV Serotypes 1–9 Mediated Gene Expression and Tropism in Mice After Systemic Injection. Mol. Ther. *16*, 1073–1080. https://doi.org/10.1038/mt.2008.76.

20. Vassalli, G., Büeler, H., Dudler, J., von Segesser, L.K., and Kappenberger, L. (2003). Adeno-associated virus (AAV) vectors achieve prolonged transgene expression in mouse myocardium and arteries *in vivo*: a comparative study with adenovirus vectors. Int. J. Cardiol. *90*, 229–238. https://doi.org/10.1016/s0167-5273(02)00554-5.

21. Shirley, J.L., de Jong, Y.P., Terhorst, C., and Herzog, R.W. (2020). Immune Responses to Viral Gene Therapy Vectors. Mol. Ther. *28*, 709–722. https://doi.org/10.1016/j.ymthe.2020.01.001.

22. Wolf, D.A., Banerjee, S., Hackett, P.B., Whitley, C.B., McIvor, R.S., and Low, W.C. (2015). Gene Therapy for Neurologic Manifestations of Mucopolysaccharidoses. Expet Opin. Drug Deliv. *12*, 283–296. https://doi.org/10.1517/17425247.2015.966682.

23. Foust, K.D., Nurre, E., Montgomery, C.L., Hernandez, A., Chan, C.M., and Kaspar, B.K. (2009). Intravascular AAV9 preferentially targets neonatal neurons and adult astrocytes. Nat. Biotechnol. *27*, 59–65. https://doi.org/10.1038/nbt.1515.

24. Li, C., and Samulski, R.J. (2020). Engineering adeno-associated virus vectors for gene therapy. Nat. Rev. Genet. *21*, 255–272. https://doi.org/10.1038/s41576-019-0205-4.

25. Cardone, M., Polito, V.A., Pepe, S., Mann, L., D'Azzo, A., Auricchio, A., Ballabio, A., and Cosma, M.P. (2006). Correction of Hunter syndrome in the MPSII mouse model by AAV2/8-mediated gene delivery. Hum. Mol. Genet. *15*, 1225–1236. https://doi.org/10.1093/hmg/ddl038.

26. Polito, V.A., and Cosma, M.P. (2009). IDS Crossing of the Blood-Brain Barrier Corrects CNS Defects in MPSII Mice. Am. J. Hum. Genet. *85*, 296–301. https://doi.org/10.1016/j.ajhg.2009.07.011.

27. Fu, H., Zaraspe, K., Murakami, N., Meadows, A.S., Pineda, R.J., McCarty, D.M., and Muenzer, J. (2018). Targeting Root Cause by Systemic scAAV9-hIDS Gene Delivery: Functional Correction and Reversal of Severe MPS II in Mice. Mol. Ther. Methods Clin. Dev. *10*, 327–340. https://doi.org/10.1016/j.omtm.2018.07.005.

28. Laoharawee, K., Podetz-Pedersen, K.M., Nguyen, T.T., Evenstar, L.B., Kitto, K.F., Nan, Z., Fairbanks, C.A., Low, W.C., Kozarsky, K.F., and McIvor, R.S. (2017). Prevention of Neurocognitive Deficiency in Mucopolysaccharidosis Type II Mice by Central Nervous System–Directed, AAV9-Mediated Iduronate Sulfatase Gene Transfer. Hum. Gene Ther. *28*, 626–638. https://doi.org/10.1089/hum.2016.184.

29. Hinderer, C., Katz, N., Louboutin, J.-P., Bell, P., Yu, H., Nayal, M., Kozarsky, K., O'Brien, W.T., Goode, T., and Wilson, J.M. (2016). Delivery of an Adeno-Associated Virus Vector into Cerebrospinal Fluid Attenuates Central Nervous System Disease in Mucopolysaccharidosis Type II Mice. Hum. Gene Ther. *27*, 906–915. https://doi.org/10.1089/hum.2016.101.

30. Motas, S., Haurigot, V., Garcia, M., Marcó, S., Ribera, A., Roca, C., Sánchez, X., Sánchez, V., Molas, M., Bertolin, J., et al. (2016). CNS-directed gene therapy for the treatment of neurologic and somatic mucopolysaccharidosis type II (Hunter syndrome). JCI Insight *1*, e86696. https://doi.org/10.1172/jci.insight.86696.

31. Harmatz, P., Prada, C.E., Burton, B.K., Lau, H., Kessler, C.M., Cao, L., Falaleeva, M., Villegas, A.G., Zeitler, J., Meyer, K., et al. (2022). First-in-human *in vivo* genome editing via AAV-zinc finger nucleases for mucopolysaccharidosis I/II and hemophilia B. Mol. Ther. *30*, 3587–3600. https://doi.org/10.1016/j.ymthe.2022.10.010.

32. Braun, S.E., Pan, D., Aronovich, E.L., Jonsson, J.J., McIvor, R.S., and Whitley, C.B. (1996). Preclinical Studies of Lymphocyte Gene Therapy for Mild Hunter Syndrome (Mucopolysaccharidosis Type II). Hum. Gene Ther. *7*, 283–290. https://doi.org/10.1089/hum.1996.7.3-283.

33. Whitley, C.B., McIvor, R.S., Aronovich, E.L., Berry, S.A., Blazar, B.R., Burger, S.R., Kersey, J.H., King, R.A., Faras, A.J., Latchaw, R.E., et al. (1996). Retroviral-Mediated Transfer of the Iduronate-2-Sulfatase Gene into Lymphocytes for Treatment of Mild Hunter Syndrome (Mucopolysaccharidosis Type II). Hum. Gene Ther. *7*, 537–549. https://doi.org/10.1089/hum.1996.7.4-537.

34. Laoharawee, K., Podetz-Pedersen, K.M., Nguyen, T.T., Singh, S.M., Smith, M.C., Belur, L.R., Low, W.C., Kozarsky, K.F., and McIvor, R.S. (2023). Non-invasive intravenous administration of AAV9 transducing iduronate sulfatase leads to global metabolic correction and prevention of neurologic deficits in a mouse model of Hunter syndrome. Mol. Genet. Metab. Rep. *34*, 100956. https://doi.org/10.1016/j.ymgmr.2023.100956.

35. Laoharawee, K., DeKelver, R.C., Podetz-Pedersen, K.M., Rohde, M., Sproul, S., Nguyen, H.-O., Nguyen, T., St Martin, S.J., Ou, L., Tom, S., et al. (2018). Dose-Dependent Prevention of Metabolic and Neurologic Disease in Murine MPS II by ZFN-Mediated In Vivo Genome Editing. Mol. Ther. *26*, 1127–1136. https://doi.org/10.1016/j.ymthe.2018.03.002.

36. Garcia, A.R., Pan, J., Lamsa, J.C., and Muenzer, J. (2007). The characterization of a murine model of mucopolysaccharidosis II (Hunter syndrome). J. Inherit. Metab. Dis. *30*, 924–934. https://doi.org/10.1007/s10545-007-0641-8.

37. Meikle, P.J., Brooks, D.A., Ravenscroft, E.M., Yan, M., Williams, R.E., Jaunzems, A.E., Chataway, T.K., Karageorgos, L.E., Davey, R.C., Boulter, C.D., et al. (1997). Diagnosis of lysosomal storage disorders: evaluation of lysosome-associated membrane protein LAMP-1 as a diagnostic marker. Clin. Chem. *43*, 1325–1335. https://doi.org/10.1093/clinchem/43.8.1325.

38. Han, S.-O., Gheorghiu, D., Li, S., Kang, H.R., and Koeberl, D. (2022). Minimum Effective Dose to Achieve Biochemical Correction with Adeno-Associated Virus Vector-Mediated Gene Therapy in Mice with Pompe Disease. Hum. Gene Ther. *33*, 492–498. https://doi.org/10.1089/hum.2021.252.

39. Mingozzi, F., and High, K.A. (2013). Immune responses to AAV vectors: overcoming barriers to successful gene therapy. Blood *122*, 23–36. https://doi.org/10.1182/blood-2013-01-306647.

40. Jiang, H., Couto, L.B., Patarroyo-White, S., Liu, T., Nagy, D., Vargas, J.A., Zhou, S., Scallan, C.D., Sommer, J., Vijay, S., et al. (2006). Effects of transient immunosuppression on adenoassociated, virus-mediated, liver-directed gene transfer in rhesus macaques and implications for human gene therapy. Blood *108*, 3321–3328. https://doi.org/10.1182/blood-2006-04-017913.

41. Murphy, S.L., Li, H., Zhou, S., Schlachterman, A., and High, K.A. (2008). Prolonged Susceptibility to Antibody-mediated Neutralization for Adeno-associated Vectors Targeted to the Liver. Mol. Ther. *16*, 138–145. https://doi.org/10.1038/sj.mt.6300334.

42. Scallan, C.D., Jiang, H., Liu, T., Patarroyo-White, S., Sommer, J.M., Zhou, S., Couto, L.B., and Pierce, G.F. (2006). Human immunoglobulin inhibits liver transduction by AAV vectors at low AAV2 neutralizing titers in SCID mice. Blood *107*, 1810–1817. https://doi.org/10.1182/blood-2005-08-3229.

43. Zhu, J., Huang, X., and Yang, Y. (2009). The TLR9-MyD88 pathway is critical for adaptive immune responses to adeno-associated virus gene therapy vectors in mice. J. Clin. Invest. *119*, 2388–2398. https://doi.org/10.1172/JCI37607.

44. Zaiss, A.K., Cotter, M.J., White, L.R., Clark, S.A., Wong, N.C.W., Holers, V.M., Bartlett, J.S., and Muruve, D.A. (2008). Complement Is an Essential Component of the Immune Response to Adeno-Associated Virus Vectors. J. Virol. *82*, 2727–2740. https://doi.org/10.1128/JVI.01990-07.

45. Bobo, T.A., Samowitz, P.N., Robinson, M.I., and Fu, H. (2020). Targeting the Root Cause of Mucopolysaccharidosis IIIA with a New scAAV9 Gene Replacement Vector. Mol. Ther. Methods Clin. Dev. *19*, 474–485. https://doi.org/10.1016/j.omtm.2020.10.014.

46. Fu, H., DiRosario, J., Killedar, S., Zaraspe, K., and McCarty, D.M. (2011). Correction of Neurological Disease of Mucopolysaccharidosis IIIB in Adult Mice by rAAV9 Trans-Blood–Brain Barrier Gene Delivery. Mol. Ther. *19*, 1025–1033. https://doi.org/10.1038/mt.2011.34.

47. Hinderer, C., Bell, P., Gurda, B.L., Wang, Q., Louboutin, J.-P., Zhu, Y., Bagel, J., O'Donnell, P., Sikora, T., Ruane, T., et al. (2014). Intrathecal Gene Therapy Corrects CNS Pathology in a Feline Model of Mucopolysaccharidosis I. Mol. Ther. *22*, 2018–2027. https://doi.org/10.1038/mt.2014.135.

48. Malato, Y., Naqvi, S., Schürmann, N., Ng, R., Wang, B., Zape, J., Kay, M.A., Grimm, D., and Willenbring, H. (2011). Fate tracing of mature hepatocytes in mouse liver homeostasis and regeneration. J. Clin. Invest. *121*, 4850–4860. https://doi.org/10.1172/JCI59261.

49. Manno, C.S., Pierce, G.F., Arruda, V.R., Glader, B., Ragni, M., Rasko, J.J., Ozelo, M.C., Hoots, K., Blatt, P., Konkle, B., et al. (2006). Successful transduction of liver in hemophilia by AAV-Factor IX and limitations imposed by the host immune response. Nat. Med. *12*, 342–347. https://doi.org/10.1038/nm1358.

50. Ertl, H.C.J. (2021). T Cell-Mediated Immune Responses to AAV and AAV Vectors. Front. Immunol. *12*, 666666.

51. Berns, K.I., and Muzyczka, N. (2017). AAV: An Overview of Unanswered Questions. Hum. Gene Ther. *28*, 308–313. https://doi.org/10.1089/hum.2017.048.

52. Nguyen, G.N., Everett, J.K., Kafle, S., Roche, A.M., Raymond, H.E., Leiby, J., Wood, C., Assenmacher, C.-A., Merricks, E.P., Long, C.T., et al. (2021). A long-term study of AAV gene therapy in dogs with hemophilia A identifies clonal expansions of transduced liver cells. Nat. Biotechnol. *39*, 47–55. https://doi.org/10.1038/s41587-020-0741-7.

53. George, L.A., Monahan, P.E., Eyster, M.E., Sullivan, S.K., Ragni, M.V., Croteau, S.E., Rasko, J.E.J., Recht, M., Samelson-Jones, B.J., MacDougall, A., et al. (2021). Multiyear Factor VIII Expression after AAV Gene Transfer for Hemophilia. N. Engl. J. Med. *385*, 1961–1973. https://doi.org/10.1056/NEJMoa2104205.

54. Gleitz, H.F., Liao, A.Y., Cook, J.R., Rowlston, S.F., Forte, G.M., D'Souza, Z., O'Leary, C., Holley, R.J., and Bigger, B.W. (2018). Brain-targeted stem cell gene therapy corrects mucopolysaccharidosis type II via multiple mechanisms. EMBO Mol. Med. *10*, e8730. https://doi.org/10.15252/emmm.201708730.

55. Schuster, D.J., Dykstra, J.A., Riedl, M.S., Kitto, K.F., Belur, L.R., McIvor, R.S., Elde, R.P., Fairbanks, C.A., and Vulchanova, L. (2014). Biodistribution of adeno-associated virus serotype 9 (AAV9) vector after intrathecal and intravenous delivery in mouse. Front. Neuroanat. *8*, 42. https://doi.org/10.3389/fnana.2014.00042.

56. Belur, L.R., Podetz-Pedersen, K.M., Tran, T.A., Mesick, J.A., Singh, N.M., Riedl, M., Vulchanova, L., Kozarsky, K.F., and McIvor, R.S. (2020). Intravenous delivery for treatment of mucopolysaccharidosis type I: A comparison of AAV serotypes 9 and rh10. Mol. Genet. Metab. Rep. *24*, 100604. https://doi.org/10.1016/j.ymgmr.2020.100604.

57. Ou, L., Przybilla, M.J., Ahlat, O., Kim, S., Overn, P., Jarnes, J., O'Sullivan, M.G., and Whitley, C.B. (2020). A Highly Efficacious PS Gene Editing System Corrects Metabolic and Neurological Complications of Mucopolysaccharidosis Type I. Mol. Ther. *28*, 1442–1454. https://doi.org/10.1016/j.ymthe.2020.03.018.

58. Ou, L., Herzog, T., Koniar, B.L., Gunther, R., and Whitley, C.B. (2014). High-dose enzyme replacement therapy in murine Hurler syndrome. Mol. Genet. Metabol. *111*, 116–122. https://doi.org/10.1016/j.ymgme.2013.09.008.

59. Aronovich, E.L., Bell, J.B., Khan, S.A., Belur, L.R., Gunther, R., Koniar, B., Schachern, P.A., Parker, J.B., Carlson, C.S., Whitley, C.B., et al. (2009). Systemic Correction of Storage Disease in MPS I NOD/SCID Mice Using the Sleeping Beauty Transposon System. Mol. Ther. *17*, 1136–1144. https://doi.org/10.1038/mt.2009.87.

60. Wada, M., Shimada, Y., Iizuka, S., Ishii, N., Hiraki, H., Tachibana, T., Maeda, K., Saito, M., Arakawa, S., Ishimoto, T., et al. (2020). Ex Vivo Gene Therapy Treats Bone Complications of Mucopolysaccharidosis Type II Mouse Models through Bone Remodeling Reactivation. Mol. Ther. Methods Clin. Dev. *19*, 261–274. https://doi.org/10.1016/j.omtm.2020.09.012.

61. Smith, M.C., Belur, L.R., Karlen, A.D., Erlanson, O., Podetz-Pedersen, K.M., McKenzie, J., Detellis, J., Gagnidze, K., Parsons, G., Robinson, N., et al. (2022). Phenotypic Correction of Murine Mucopolysaccharidosis Type II by Engraftment of Ex Vivo Lentiviral Vector-Transduced Hematopoietic Stem and Progenitor Cells. Hum. Gene Ther. *33*, 1279–1292. https://doi.org/10.1089/hum.2022.141.

62. Belur, L.R., Romero, M., Lee, J., Podetz-Pedersen, K.M., Nan, Z., Riedl, M.S., Vulchanova, L., Kitto, K.F., Fairbanks, C.A., Kozarsky, K.F., et al. (2021). Comparative Effectiveness of Intracerebroventricular, Intrathecal, and Intranasal Routes of AAV9 Vector Administration for Genetic Therapy of Neurologic Disease in Murine Mucopolysaccharidosis Type I. Front. Mol. Neurosci. *14*, 618360. https://doi.org/10.3389/fnmol.2021.618360.

63. Au, H.K.E., Isalan, M., and Mielcarek, M. (2022). Gene Therapy Advances: A Meta-Analysis of AAV Usage in Clinical Settings. Front. Med. *8*, 809118. https://doi.org/10.3389/fmed.2021.809118.

64. Paulk, N. (2020). Gene Therapy: It Is Time to Talk about High-Dose AAV. Genet. Eng. Biotechnol. News *40*, 14–16. https://doi.org/10.1089/gen.40.09.04.

65. Wilson, J.M., and Flotte, T.R. (2020). Moving Forward After Two Deaths in a Gene Therapy Trial of Myotubular Myopathy. Hum. Gene Ther. *31*, 695–696. https://doi.org/10.1089/hum.2020.182.

66. Nathwani, A.C., Tuddenham, E.G.D., Rangarajan, S., Rosales, C., McIntosh, J., Linch, D.C., Chowdary, P., Riddell, A., Pie, A.J., Harrington, C., et al. (2011). Adenovirus-Associated Virus Vector–Mediated Gene Transfer in Hemophilia B. N. Engl. J. Med. *365*, 2357–2365. https://doi.org/10.1056/NEJMoa1108046.

67. Nathwani, A.C., Reiss, U.M., Tuddenham, E.G.D., Rosales, C., Chowdary, P., McIntosh, J., Della Peruta, M., Lheriteau, E., Patel, N., Raj, D., et al. (2014). Long-Term Safety and Efficacy of Factor IX Gene Therapy in Hemophilia B. N. Engl. J. Med. *371*, 1994–2004. https://doi.org/10.1056/NEJMoa1407309.

68. Montaño, A.M., Lock-Hock, N., Steiner, R.D., Graham, B.H., Szlago, M., Greenstein, R., Pineda, M., Gonzalez-Meneses, A., Çoker, M., Bartholomew, D., et al. (2016). Clinical course of sly syndrome (mucopolysaccharidosis type VII). J. Med. Genet. *53*, 403–418. https://doi.org/10.1136/jmedgenet-2015-103322.

69. Stirnemann, J., Belmatoug, N., Camou, F., Serratrice, C., Froissart, R., Caillaud, C., Levade, T., Astudillo, L., Serratrice, J., Brassier, A., et al. (2017). A Review of Gaucher Disease Pathophysiology, Clinical Presentation and Treatments. Int. J. Mol. Sci. *18*, 441. https://doi.org/10.3390/ijms18020441.

70. Cenacchi, G., Papa, V., Pegoraro, V., Marozzo, R., Fanin, M., and Angelini, C. (2020). Review: Danon disease: Review of natural history and recent advances. Neuropathol. Appl. Neurobiol. *46*, 303–322. https://doi.org/10.1111/nan.12587.

71. Piechnik, M., Amendum, P.C., Sawamoto, K., Stapleton, M., Khan, S., Fnu, N., Álvarez, V., Pachon, A.M.H., Danos, O., Bruder, J.T., et al. (2022). Sex Difference Leads to Differential Gene Expression Patterns and Therapeutic Efficacy in Mucopolysaccharidosis IVA Murine Model Receiving AAV8 Gene Therapy. Int. J. Mol. Sci. *23*, 12693. https://doi.org/10.3390/ijms232012693.

72. Hylden, J.L., and Wilcox, G.L. (1980). Intrathecal morphine in mice: A new technique. Eur. J. Pharmacol. *67*, 313–316. https://doi.org/10.1016/0014-2999(80)90515-4.

73. Fairbanks, C.A. (2003). Spinal delivery of analgesics in experimental models of pain and analgesia. Adv. Drug Deliv. Rev. *55*, 1007–1041. https://doi.org/10.1016/S0169-409X(03)00101-7.

74. Voznyi, Y.V., Keulemans, J.L., and van Diggelen, O.P. (2001). A fluorimetric enzyme assay for the diagnosis of MPS II (Hunter disease). J. Inherit. Metab. Dis. *24*, 675–680. https://doi.org/10.1023/A:1012763026526.

75. Barnes, C.A. (1979). Memory deficits associated with senescence: a neurophysiological and behavioral study in the rat. J. Comp. Physiol. Psychol. *93*, 74–104. https://doi.org/10.1037/h0077579.